ELSEVIER

Contents lists available at ScienceDirect

BBA - Molecular Cell Research

journal homepage: www.elsevier.com/locate/bbamcr



Research Paper

Effects of CDC45 mutations on DNA replication and genome stability

Milena Denkiewicz-Kruk¹, Deepali Chaudhry¹, Alina Krasilia, Malgorzata Jedrychowska, Iwona J. Fijalkowska^{*}, Michal Dmowski^{*}

Institute of Biochemistry and Biophysics Polish Academy of Sciences, Pawinskiego 5a, 02-106 Warsaw, Poland

ARTICLE INFO

Keywords: CDC45 CMG helicase Polymerase zeta DRIM Mismatch repair DNA replication fidelity Meier-Gorlin syndrome MGGRS

ABSTRACT

Cdc45 is a non-catalytic subunit of the CMG helicase complex that is recruited to the autonomously replicating sequence at the onset of DNA replication. The Cdc45 protein is required for the initiation of DNA replication as well as for nascent DNA strand synthesis. It interacts with Mcm2 and Psf1 elements of CMG helicase, as well as with Sld3, an initiation factor, and Pol2, the catalytic subunit of DNA polymerase epsilon (Pol e). In this study, we analyzed the effects of amino acid substitutions in the Cdc45 region involved in the interaction of this protein with Mcm2–7 (Cdc45-1), Psf1 (Cdc45-26), and Sld3 (Cdc45-25, Cdc45-35). We found that mutations in CDC45 resulted in defective DNA replication. Under permissive conditions, delayed DNA synthesis was observed. At restrictive temperatures, the mutant cells were unable to efficiently replicate DNA. However, after the initiation of DNA replication under permissive conditions, the four analyzed CDC45 mutants exhibited DNA synthesis under the restrictive conditions. Moreover, we observed increased mutation rates, mainly dependent on DNA polymerase zeta (Pol ζ), as well as increased incidence of replication errors. These findings confirm the essential function of Cdc45 in DNA replication initiation and demonstrate that impaired Cdc45 subunit has an impact on the fidelity of the nascent DNA strand synthesis. The changes in cell function observed in this study, related to defects in Cdc45 function, may help understand some diseases associated with CDC45.

1. Introduction

Faithful replication of genetic information is crucial for maintaining genomic stability. This requires the coordinated action of many catalytic and non-catalytic proteins during initiation, elongation, and termination of DNA replication. In the first step of initiation, the six-subunit protein complex Orc1-6 (origin recognition complex) binds to the ARS (autonomously replicating sequence) [1]. Subsequently, Cdc6 and Cdt1 proteins attach to two Mcm2-7 heterohexamer complexes (inactive helicase cores), which together form the pre-Replicative Complex (pre-RC) [2]. In parallel, the Sld3-Sld7 complex binds to the Cdc45 protein [3]. After phosphorylation of the Mcm2-7 heterohexamer by DDK kinase (Dbf4-dependent kinase), the Sld3-Sld7-Cdc45 complex is recruited to the pre-RC complex [4,5]. Finally, under the control of cyclin-dependent kinases (CDKs), at the transition of G1/S phases of the cell cycle, the pre-Loading Complex (pre-LC) composed of Dpb11, Sld2, GINS, and DNA polymerase epsilon (Pol ε) binds to the pre-RC, resulting in the formation of the pre-Initiation Complex (pre-IC). After forming the pre-IC, the Dpb11, Sld2, Sld3, and Sld7 proteins dissociate from the complex. As a result, the active CMG helicase consists of 11 proteins: the Cdc45 protein, the Mcm2–7 heterohexamer, and the GINS heterotetramer (Psf1–3, Sld5) [6] which, through interaction with Pol ϵ , form an active fifteen-subunit CMGE complex that unwinds the DNA double helix (CMG helicase) and replicates the leading strand (Pol ϵ) [7]. During the unwinding of double-stranded DNA by CMG helicase, Replication Protein A (RPA) binds to and protects the single-stranded DNA (ssDNA) [8].

Recent studies indicated that the non-catalytic subunits of helicase serve functions beyond their structural role and are crucial for the proper functioning of the entire replisome. Although the Cdc45 protein and the GINS complex are auxiliary subunits with no catalytic activity, they play a key role in activating CMG helicase [6,9]. In addition, Cdc45-GINS stabilizes the correct spatial structure of the Mcm2–7 complex and positions the leading DNA strand in the central channel, also preventing it from sliding out through the Mcm2/5 gate under conditions such as replication stress [10–12].

Early studies have shown that Cdc45 is essential for cell viability [13,14]. Later, it was shown that both yeast and human Cdc45 proteins

^{*} Corresponding authors.

 $[\]textit{E-mail addresses:} iwonaf@ibb.waw.pl~(I.J.~Fijalkowska),~mdmowski@ibb.waw.pl~(M.~Dmowski).$

¹ These authors contributed equally to this work.

bind to ssDNA, activating cellular responses under replication stress [15]. Initially, bioinformatic analyses have shown that Cdc45 is an ortholog of bacterial RecJ, an ssDNA exonuclease belonging to the DHH family of phosphoesterases [16,17]. This was later confirmed when human and yeast Cdc45 structures were determined [18,19]. In general, Cdc45 contains the DHH and DHHA1 domains separated by a connecting domain encompassing an unstructured region, a CMG-interacting domain (CID) for Mcm binding, and a RecJ fold (structurally related to the bacterial RecJ exonuclease [16]) involved in its interaction with Psf1 [18,20] (Fig. 1A).

Although numerous studies have provided data on the structure of Cdc45 in various organisms (Fig. 1A), a detailed analysis of the consequences of the defective functioning of Cdc45 in eukaryotic cells is lacking. In the present study, we analyzed four alleles encoding Cdc45 variants with amino acid substitutions in the DHH domain: L131P (Cdc45-25), S242P (Cdc45-35), CID domain (G367D) (Cdc45-1), and RecJ fold W481R (Cdc45-26) (Fig. 1B and C). Importantly, these amino acid substitutions are located in the Cdc45 domains that interact with the proteins Mcm2, Psf1, and Sld3 (Fig. 1B and C). The *cdc45-1* allele has been described previously [21], whereas *cdc45-25*, *cdc45-26*, and *cdc45-35* were isolated as spontaneous temperature-sensitive mutants [22].

We present data indicating that proper functioning of Cdc45 in the replisome is important for genome stability. This conclusion is based on the analysis of four cdc45 mutants that exhibit impaired progression through the S phase, elevated levels of replication errors, increased amounts of ssDNA, and more frequent contribution of the mutator Pol ζ to DNA synthesis.

Investigating the role of the Cdc45 protein is critical in light of studies describing that dysfunction of both alleles of the CDC45 gene in

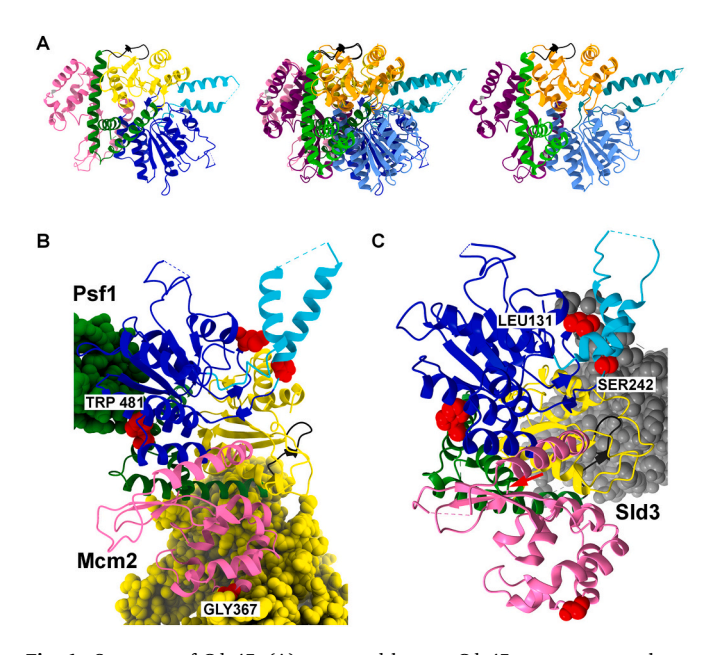


Fig. 1. Structure of Cdc45: (A) yeast and human Cdc45 structures are shown separately (left and right, respectively) and overlayed (center) based on PDB 7qhs and 7pfo [70,71]. Protein domains are shown in specific colors: blue/cornflower blue — DHH; cyan/light sea green — helical insertion with unstructured region, absent in RecJ; green/lime — RecJ fold; pink/purple — CID; yellow/orange — DHHA1; (B) structure of Cdc45 and interacting proteins Mcm2 (yellow) and Psf1 (green) based on PDB 7qhs [70]; (C) structure of Cdc45 and Sld3 (grey) based on PDB Japan 8j09 [69]. Other components of CMG were omitted for clarity. Substituted residues in Cdc45 are shown as red spheres: G367D (Cdc45-1), L131P (Cdc45-25), W481R (Cdc45-26), and S242P (Cdc45-35). Structures according to PDB 7QHS [70] and PDB 7PFO [71]. (For interpretation of the references to color in this figure legend, the reader is referred to the web version of this article.)

humans leads to the development of an autosomal recessive disease — Meier-Gorlin syndrome 7 (MGORS7, MIM #617063) [23–25], and recent studies have demonstrated a promoting role of *CDC45* in oncogenesis [26–29].

2. Materials and methods

2.1. Strains, media, and general methods

The <code>Saccharomyces cerevisiae</code> strains were grown in standard media [30]. A complete YPD medium was used when nutrition selection was not required. YPD with nourseothricin 100 μ g/mL (Werner BioAgents, Jena, Germany), or hygromycin B (BioShop Canada Inc.) and SD medium supplemented with appropriate amino acids and nitrogenous bases were used to select and propagate transformants. For the forward mutagenesis assays at the <code>CAN1</code> locus, the SD medium with appropriate amino acids and nitrogenous bases was supplemented with 60 μ g/mL <code>L-canavanine</code> (Sigma Aldrich, St. Louis, MO, USA). The SD medium with 1 mg/mL 5-fluoroorotic acid (5-FOA) (US Biological, Salem, MA, USA) was used to select cells that lost the functional <code>URA3</code> gene.

Yeast cells were transformed using the lithium acetate/single-stranded carrier DNA/PEG method [31]. Chromosomal DNA was isolated from yeast cultures using the Genomic Mini AX Yeast Spin Kit (A&A Biotechnology, Gdansk, Poland).

Escherichia coli DH5α (endA1 glnV44 thi-1 recA1 relA1 gyrA96 deoR nupG Φ80d lacZΔ M15Δ (lacZYA-argF) U₁₆₉, hsdR₁₇ (r_K^-, m_K^+), λ^-) (Invitrogen, California, United States) cells were grown at 37 °C in LB medium, supplemented, when needed, with ampicillin 100 μg/mL (Polfa Tarchomin S.A., Warsaw, Poland). *E. coli* cells were transformed as described in [32]. Bacterial plasmids were isolated using the Plasmid Mini Kit (A&A Biotechnology, Gdansk, Poland).

2.2. Construction of yeast strains

The *Saccharomyces cerevisiae* strains used in this study are derivatives of strain $\Delta I(-2)I$ -7BYUNI300 [33], detailed in Table S1.

The cdc45-1 allele has been previously described [21], while cdc45-25, cdc45-26, and cdc45-35 alleles were obtained in the Hiroyuki Araki lab (NIG, Mishima, Japan) in a search for mutations in CDC45 generating temperature-sensitive phenotype [22] (https://ir.soken.ac. jp/records/992). Yeast strains with mutated CDC45 alleles are derivatives of SC765 obtained using integration cassettes derived from YIp211cdc45-1, YIp211cdc45-26 by BglII digestion, or YIp211cdc45-25, YIp211cdc45-35 by XbaI digestion. These plasmids, obtained from Hiroyuki Araki, were constructed by subcloning 2.2 kb BamHI-HindIII fragments from YCp22CDC45-derivatives with mutated alleles [22,34] into the BamHI-HindIII sites of YIplac211. The SC765 derivatives with CDC45 alleles were selected on the SD medium without uracil. Transformants were grown at 30 °C (cdc45-1) or 23 °C (cdc45-25, cdc45-26, cdc45-35) for 5 to 7 days. Integrations of the cdc45 alleles into the CDC45 chromosomal locus were confirmed by PCR and DNA sequencing using primers cdc45_up, cdc45_dw, cdc45_1, cdc45_2, cdc45_3, cdc45_4 (Table S2). Additionally, temperature sensitivity at 37 °C for cdc45-25, cdc45-26, and cdc45-35 strains and cold sensitivity at 18 °C for the cdc45-1 strain were verified. Finally, transformants were spread onto 5-FOA plates to select cells that had lost the URA3 gene.

The *cdc45* strains (Y1050, Y1051, Y1052 and Y1053) and the *CDC45* control strain (SC765) were subjected to further modifications. For *REV3* disruption, the *rev3::LEU2* disruption cassette was used as previously described [35]. Transformants were selected for leucine prototrophy on the SD medium at 30 °C (Y1050) or 23 °C (Y1051, Y1052, and Y1053 strains) for 5 to 7 days. The integration of *rev3::LEU2* was confirmed by PCR using primers REV3 A, REV3 B, REV3 C, and REV3 D (Table S2). The *RFA1-YFP* fusion was introduced as described previously [36]. Transformants were selected on the SD medium for leucine prototrophy at 30 °C (Y1050) or 23 °C (Y1051, Y1052, and Y1053 strains)

for 5 to 7 days and verified by PCR, using primers RFA6231R, RFA7367F and YFP9451R (Table S2). For MSH2 disruption, the msh2::NAT1 disruption cassette was PCR-amplified with primers MSH_UPTEF and MSH2_DNTEF (Table S2) using pAG25 [37] as a template. Transformants were grown on a YPD medium supplemented with nourseothricin (100 $\mu g/mL$) at 30 °C (Y1050) or 23 °C (Y1051, Y1052 and Y1053 strains) for 5 to 7 days. The integration of the of msh2::NAT1 was confirmed by PCR using primers MSH2 A, MSH2 B, MSH2 C, MSH2 D, msh2_up, msh2_prdw, NAT1 UO and NAT1 DO (Table S2). The cdc45-1 $rad52\Delta$ and cdc45-1 $rad51\Delta$ strains were obtained by tetrad dissection from diploid strains constructed by crossing strains Y1050 with Y1001 or Y1002, respectively. RAD52 or RAD51 disruption was verified using PCR with primers RAD52 A, RAD52 B, RAD52 C, RAD52 D, RAD51 A, RAD51 B, RAD51 C, RAD51 D, HPH UO, and HPH DO (Table S2). For DDC1 disruption, the ddc1::HPH cassette was used as previously described [38]. Gene replacement was verified using PCR with primers UFddc1_2, DRddc1_2, DDC1UO, DDC1DO, HPH UO, and HPH DO (Table S2).

2.3. Synchronization in G1 Phase with α -Factor and HU-arrest

Strains SC765, Y1050, Y1051, Y1052 and Y1053 were grown until the OD₆₀₀ reached 0.4. Next, cells were harvested and resuspended in fresh medium supplemented with α -factor (4 μ g/mL). Additionally, α -factor (4 μ g/mL) was added after 60–90 min incubation. After 2–3 h of growth at 23 °C or 30 °C cells were harvested and washed three times with sterile water and then resuspended in fresh SD medium and released into a new cell cycle at 23 °C or 37 °C (strains SC765, Y1051, Y1052 and Y1053) and, at 30 $^{\circ}$ C or 18 $^{\circ}$ C (strains SC765 and Y1051). At indicated time points, 1 mL samples were taken. Cell pellets were resuspended in 1 mL of 70 % ethanol. For HU-arrest experiments, cells were released from the G1 block in the SD medium with hydroxyurea (200 mM) (SIGMA) at 23 °C (strains SC765, Y1051, Y1052 and Y1053) and at 30 $^{\circ}$ C (strains SC765 and Y1051) for 120 min. Next, cells were washed with sterile water and resuspended in the SD medium for incubation at 23 $^{\circ}\text{C}$ or 37 $^{\circ}\text{C}$ (strains SC765, Y1051, Y1052, and Y1053) and at 30 °C or 18 °C (strains SC765 and Y1051). At indicated time points, 1 mL samples were taken. Cell pellets were resuspended in 1 mL of 70 % ethanol.

2.4. Flow cytometry analysis

Samples were taken from at least three replicates and prepared for flow cytometry, as described previously [38], with modifications according to specific strain requirements. Yeast cells were stained using SYTOX Green (0.5 μ M) (Invitrogen, Carlsbad, CA, USA). The DNA content was determined by measuring the SYTOX Green fluorescence signal (FL1) using Becton Dickinson FACSCalibur and CellQuest software (BD Bioscience, San Jose, CA, United States). Further analyses including calculation of the number of cells in specific cell cycle phases were done using Flowing Software (https://flowingsoftware.com/). The significance of observed differences in cell populations was verified using multiple comparison unpaired t-test (Prism — GraphPad).

2.5. Measurement of spontaneous mutation rates

To determine spontaneous mutation rates, 10 to 20 cultures of 2 or 3 independent isolates of each strain were inoculated in 2.5 mL (*CAN1* locus) or 20 mL (*his7-2* locus) of liquid SD medium, supplemented with the required amino acids and nitrogenous bases. Cultures were grown at 23 °C or 30 °C until they reached the stationary phase. Then, cells were collected by centrifugation, washed, and resuspended in 0.8 % NaCl. Aliquots of concentrated cultures and their appropriate dilutions were plated on selective (containing L-canavanine 60 μ g/mL, or deprived of histidine) and nonselective media. Colonies were counted after 5–7 days of growth at 30 °C or 23 °C. Mutation rates were calculated using the

MLE MUtation Rate calculator (mlemur) [39].

2.6. Mutation spectra

A total of 192 cultures of 2 independent isolates of the Y1050 strain and 170 cultures of 2 independent isolates of the Y1060 strain were inoculated in 1 mL of liquid SD medium supplemented with the required amino acids and nitrogenous bases, lacking leucine, and grown at 30 °C. When cultures reached the stationary phase, appropriate dilutions were plated on a solid SD medium supplemented with L-canavanine (60 µg/mL). After five days of incubation at 30 °C, total DNA from a single CAN^R colony from each culture of Y1050 and Y1060 strains was isolated and used for PCR amplification of the *CAN1* locus with primers MGCANFF and MGCANRR followed by DNA sequencing with primers Can_1666, Can_1963, Can_2241, and Can_2465 (Table S2). This enabled the identification of mutations in the *CAN1* gene from CAN^R cells. For statistical analysis, a contingency table and the χ^2 test were used.

2.7. Identification of Rfa1 foci by fluorescence microscopy

Cells with *RFA1-YFP* fusion were cultured at 23 °C or 30 °C in the SD medium supplemented with the required amino acids and nitrogenous bases, excluding leucine, until they reached the exponential growth phase before samples for fluorescent microscopy were taken. Images were taken using the Axio Imager M2 fluorescence microscope with the AxioCam MRc5 Digital Camera (Zeiss, Oberkochen, Germany) and analyzed with Axio Vision 4.8 software. The number of cells and Rfa1 foci in the cells was counted. Eight biological replicates were analyzed, with over 1700 cells for each genotype. For statistical analysis, a multiple comparison unpaired *t*-test was applied (Prism — GraphPad).

3. Results

3.1. DNA replication defects in CDC45 mutant cells

We constructed mutant derivatives of the haploid $\Delta I(-2)I$ -7B-YUNI300 *Saccharomyces cerevisiae* strain with chromosomal cdc45-1, cdc45-25, cdc45-26, and cdc45-35 alleles (Table S1) encoding amino acid substitutions in the CID domain (G367D; Cdc45-1), DHH domain L131P (Cdc45-25), S242P (Cdc45-35), and the RecJ fold W481R (Cdc45-26) (Fig. 1B and C). As previous studies have shown that these replication mutants are unable to grow at specific temperatures [21,22], the resulting strains were tested for growth at 18, 23, 30, and 37 °C (Fig. S1). The strain carrying the cdc45-1 allele did not grow at 18 °C, consistent with previous studies [21]. Yeast cells carrying cdc45-25, cdc45-26, and cdc45-35 alleles did not grow at 37 °C (Fig. S1).

First, we used flow cytometry to analyze the DNA content profile of cdc45 mutant strains at permissive temperatures of 30 °C for cdc45-1 and 23 °C for cdc45-25, cdc45-26, and cdc45-35 cells. This approach facilitates the estimation of the relative number of cells in the G1, S, and G2/M phases of the cell cycle. The results presented in Fig. 2 show that in an asynchronous population of wild-type cells at 30 °C, only approximately 10 % of cells are in the S phase, whereas in the cdc45-1 mutant, under the same conditions, >25 % of cells are synthesizing DNA (Fig. 2A and B). At 23 °C, roughly 13 % of the cells are in the S phase in a population of asynchronous wild-type cells. In contrast, in mutant cells with cdc45-25, cdc45-26, or cdc45-35 alleles, DNA replicating cells constitute 25 %–31 % of the population (Fig. 2C and D).

Next, we performed a time-course analysis of cell cycle progression of cells with *cdc45-1*, *cdc45-25*, *cdc45-26*, and *cdc45-35* alleles and compared them with the wild-type strain. Yeast cultures were first synchronized in the G1 phase and released into a new cell cycle at a permissive temperature (Fig. 3). Entry into a new cell cycle, i.e., into the S phase, was monitored using flow cytometry-based analysis of DNA content. A detailed statistical analysis of the results from Fig. 3 is shown in Fig. 4. At 30 °C, wild-type cells (shown in black) started DNA

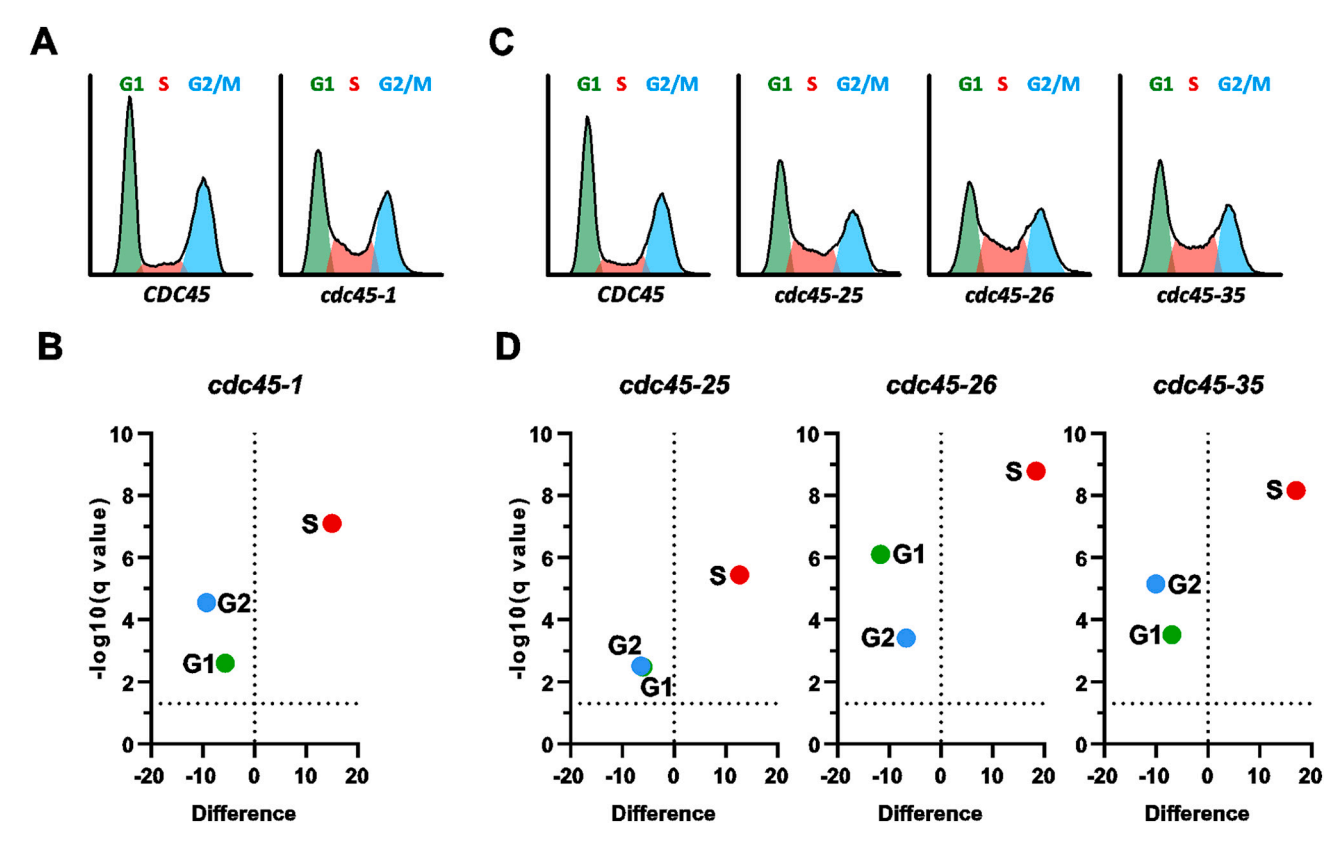


Fig. 2. Flow cytometry analysis of DNA content in *CDC45* mutant cells under permissive conditions. DNA content was analyzed in asynchronous populations of cdc45-1 mutant at 30 °C (A) or cdc45-25, cdc45-26, and cdc45-35 at 23 °C (C). The DNA content is shown on the x-axis, and the cell count is shown on the y-axis. The statistical significance of differences between mutant and wild-type strains was assessed using a multiple comparison unpaired t-test calculated for four independent repeats (B) and (D). The horizontal dotted line shows q = 0.05.

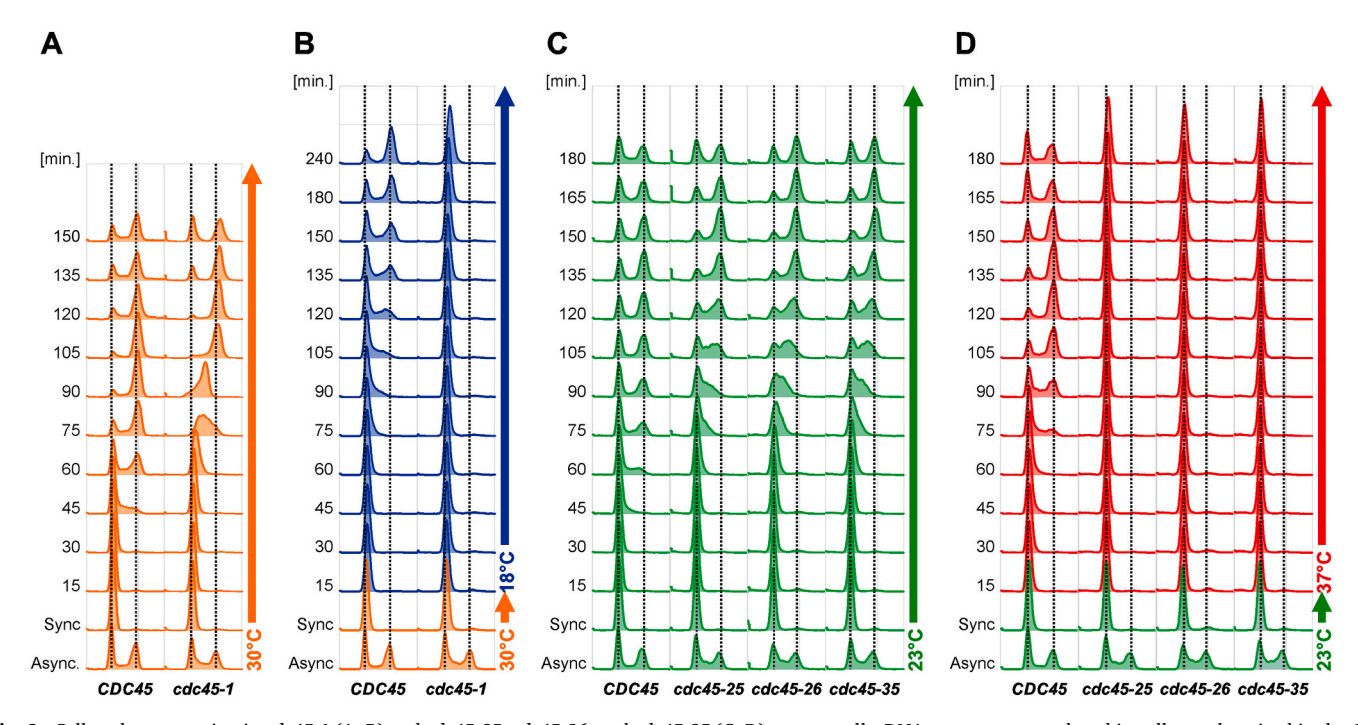
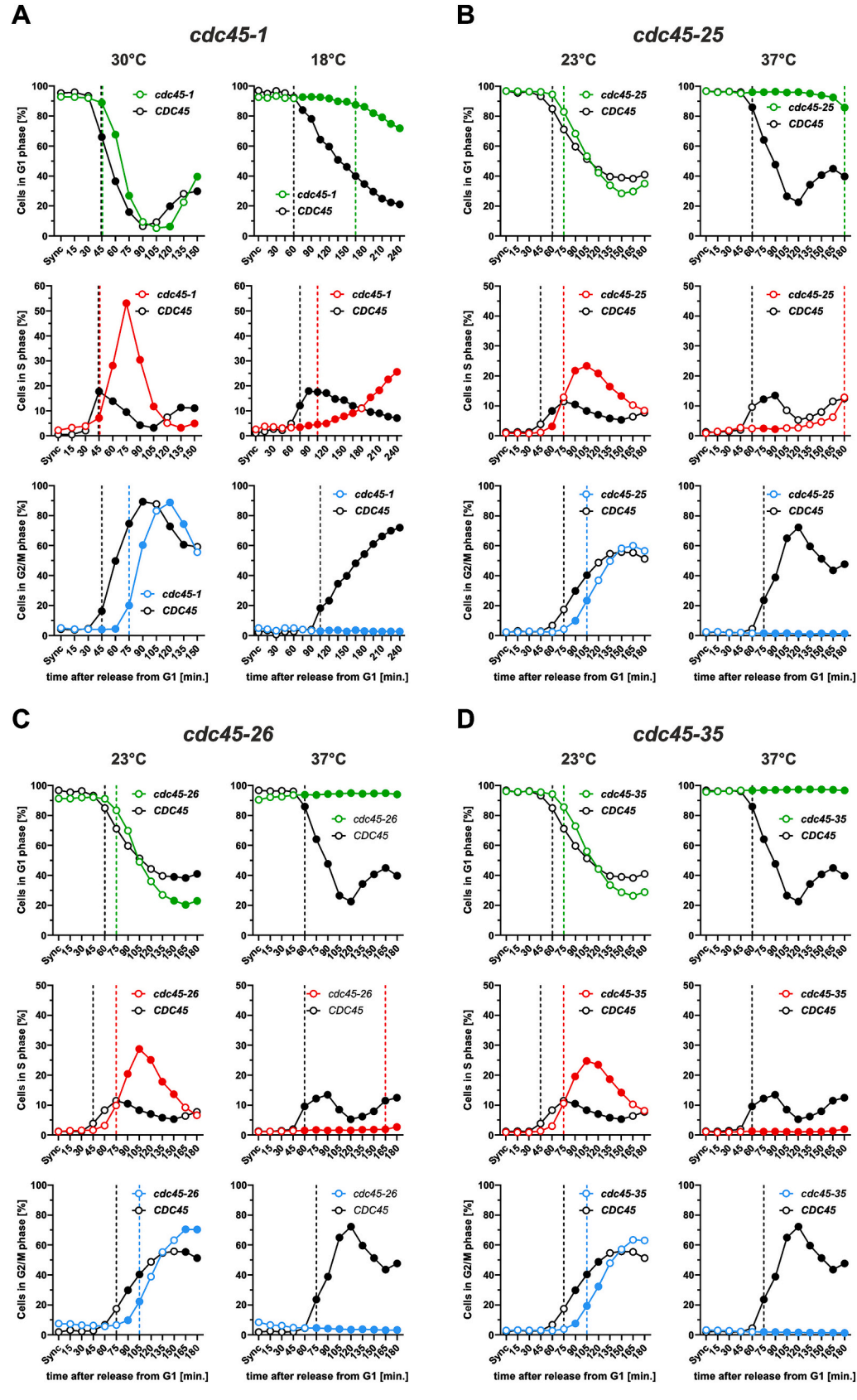


Fig. 3. Cell cycle progression in *cdc45-1* (A, B) and *cdc45-25*, *cdc45-26*, and *cdc45-35* (C, D) mutant cells. DNA content was analyzed in cells synchronized in the G1 phase and released into a new cell cycle. Cells were synchronized at the permissive temperature and released into a new cell cycle at the same temperature (30 °C in A and 23 °C in C) or restrictive temperature (18 °C in B and 37 °C in D). Samples were taken at indicated time points. More detailed analyzes are shown in Fig. 4.



(caption on next page)

Fig. 4. Cell cycle progression analysis of cdc45-1 (A), cdc45-25 (B), cdc45-26 (C), and cdc45-35 (D) cells at permissive and restrictive temperatures synchronized with α-factor before new cell cycle entry. The analysis is based on flow cytometry profiles shown in Fig. 3. The number of cell in G1, S, and G2/M phases of the cell cycle were calculated for cells synchronized in G1 phase (Sync) and released into a new cell cycle. Samples were taken at indicated time points. Average values were calculated from at least three experiments. Each value is represented by a circle: open circles represent values with no significant differences for the two compared genotypes. Closed circles represent significantly different values ($p \le 0.05$). Dashed lines, colored according to the represented genotype, indicate time points, where the value is significantly different from the value observed at the time of G1 synchronization (Sync). The significance of observed differences was analyzed using a multiple comparison unpaired t-test.

synthesis 45 min after release from the G1 block (Figs. 3A and 4A). At this time point, the population demonstrated the highest number of cells in the S phase, which then decreased rapidly. After 45 min, the cells entered the G2 phase (Figs. 3A and 4A). Subsequently, 105–120 min after the release from synchronization, wild-type cells began to divide. Under the same conditions, cells with the cdc45-1 mutation started G1 phase exit and S phase entry 45 min after release from α factor, similarly to wild-type cells. However, this transition was slower, resulting in significantly higher numbers of cells in the G1 phase and higher numbers of cells in the S phase at the 60 and 75 min time points (up to 50 %) (Fig. 4A). The slow progression through the S phase resulted in delayed entry into the G2 phase; cdc45-1 cells entered the G2 phase at the 75 min time point, compared with 45 min for wild-type cells.

A similar analysis of cells with *cdc45-25*, *cdc45-26*, and *cdc45-35* alleles and the control strain showed that, at 23 °C, DNA replication in wild-type cells started 45–60 min after release from the G1 block (Figs. 3C and 4B). A significant increase of G2 phase cells number was observed at 75 and 90 min. In contrast, in *cdc45-25*, *cdc45-26*, and *cdc45-35* mutant cells, DNA synthesis began after 75 min (Figs. 3C and 4B–D). They progressed slowly through the S phase, with the highest number of cells in S phase (20–30 %) at time point 105 and 120 min). Cells of the three temperature-sensitive mutants entered the G2 phase with a 30 min delay compared to wild-type cells (time point 105) (Fig. 4B–D).

The temperature sensitivity of the replication mutants results from their inability to replicate DNA at restrictive temperatures. Therefore, we verified whether CDC45 mutant cells could synthesize DNA at restrictive temperature during the first cell cycle after the temperature switch. For this purpose, yeast cells with mutated CDC45 alleles were synchronized in the G1 phase at a permissive temperature (30 °C for cdc45-1 and 23 $^{\circ}$ C for cdc45-25, cdc45-26, and cdc45-35) and released into a new cell cycle at the restrictive temperature (18 °C for cdc45-1 and 30 °C for cdc45-25, cdc45-26, and cdc45-35) (Fig. 3B and D). At 18 °C, wild-type cells started DNA synthesis 60-75 min after release from G1 block. The first cells entered the G2 phase after 105 min (Figs. 3B and 4A). Under the same conditions, the DNA content cdc45-1 in mutant cells barely changed; a significant change in the G1-phase cell number was observed 165 min after release from the G1 block (120 min later than in wild-type cells) (Fig. 4A). Although the cells initiated DNA synthesis, they were unable to reach the G2-phase DNA content even 240 min after release from the G1 block (Fig. 3B and 4A).

At 37 °C, in wild-type cells, DNA synthesis started 60 min after release from the G1 block (Figs. 3D and 4B). Next, 15 min later, after a fast transition through the S phase, wild-type cells entered the G2 before division, which occurred 120 min after release from synchronization in the G1 phase (Figs. 3D and 4B). In contrast, *cdc45-25*, *cdc45-26*, and *cdc45-35* mutant cells barely started DNA synthesis 180 min after G1 block release, with only a small percentage of cells showing S phase DNA content (Figs. 3D and 4B–D). Consequently, none of *cdc45-25*, *cdc45-26*, and *cdc45-35* mutant cells reached the G2 phase (Fig. 4B–D).

These results show that all the studied *CDC45* mutants encountered severe problems with DNA replication, even under permissive temperature conditions. After new cell cycle entry, *CDC45* mutant cells show a delayed start of DNA synthesis start compared with wild-type cells. Moreover, *CDC45* mutants accumulated in the S phase, reflecting slower DNA replication. At restrictive temperatures, the mutants were unable to efficiently synthesize DNA.

Cdc45 is recruited to the origin of DNA replication at the initiation

step but is also involved in the elongation of the growing DNA strand [34]. Therefore, abnormal progression through the S phase of the cell cycle may result from either defective initiation of DNA replication or inefficient replisome activity at the elongation step. To address this question, we synchronized the cells in the G1 phase. However, before releasing them into a new cell cycle, they were treated with hydroxyurea (HU) for 120 min. This compound inhibits ribonucleotide reductase and limits dNTP synthesis, which stalls DNA synthesis but does not affect the initiation steps of DNA replication and replisome assembly. At 30 $^{\circ}\text{C}$, wild-type cells started the G1-S phase transition before release from the HU treatment (Figs. 5A and 6A). Thirty minutes later, the number of G2phase cells started to increase significantly (Fig. 6A). The first daughter cells (with G1-specific DNA content) were observed 75-90 min after release from HU treatment (Fig. 6A). Under the same permissive conditions, *cdc45-1* cells, similar to the wild-type control, moved from G1 to S phase before HU depletion. Moreover, cdc45-1 cells completed the S phase only 15 min later than wild-type cells (75 versus 60 min) and initiated G2 phase entry with a similar delay (Fig. 6A). At 18 °C (under the restrictive conditions for cdc45-1), again, both wild-type and cdc45-1 mutant cells started G1 phase exit and S phase entry early after release from HU treatment (Fig. 6A); however, while wild-type cells progressed fast through the S phase and reached the G2 phase 90 min after HU removal, cdc45-1 cells hardly progressed (with up to 70 % of the cells accumulated in the S phase at 150-210 min) and started G2 phase entry with a 90 min delay compared with wild-type cells (Fig. 6A).

Interestingly, when the same experiment was performed with only 30 min of exposure to HU at the permissive temperature of 30 $^{\circ}$ C, wild-type cells started the G1-S phase transition before release from the HU treatment and mutant cells initiated G1 phase entry 15 min later (Figs. S2 and S3). Their entry into S phase and G2 phase was also similar. At 18 $^{\circ}$ C, after 30 min of exposure to HU, wild-type cells demonstrated almost identical dynamics of DNA synthesis as after 120 min exposure (Fig. S3), while cdc45-1 mutant cells started G1-S phase transition 60 min after release from HU (Fig. S3).

At 23 °C (under the permissive conditions for the three tested mutants), wild-type and cdc45-25, cdc45-26, and cdc45-35 mutant cells demonstrated almost identical dynamics of DNA synthesis. Immediately after release from HU treatment, they moved from the G1 to the S phase (Figs. 5C and 6B-D) and entered the G2 phase 60 min later. All cells reached G2-specific DNA content 105-120 min after release from the HU block (Figs. 5C and 6B–D). At the restrictive temperature of 37 °C, again, wild-type cells and cdc45-25, cdc45-26, and cdc45-35 mutant cells started G1-S transition immediately after release from HU (Figs. 5D and 6B-D). However, cdc45 mutant cells accumulated in the S phase with almost 35 %-45 % of the population showing S phase DNA content from 45 to 90 min, while wild-type cells completed the S phase within 60 min of HU release and started G2 phase entry (Fig. 6B-D). The cdc45-25, cdc45-26, and cdc45-35 mutant cells started G2-phase entry with a 15–30 min delay compared with the wild-type cells (Fig. 6B–D). This demonstrates that DNA replication initiation at the permissive temperature facilitates efficient, albeit slower, DNA synthesis in cdc45-25, cdc45-26, and cdc45-35 mutant cells, even under stressful conditions.

3.2. CDC45 mutants accumulate single-stranded DNA

Defective replisome functioning may result in discontinued DNA synthesis at one or both DNA strands and the formation of ssDNA stretches. These can subsequently be used as templates for DNA

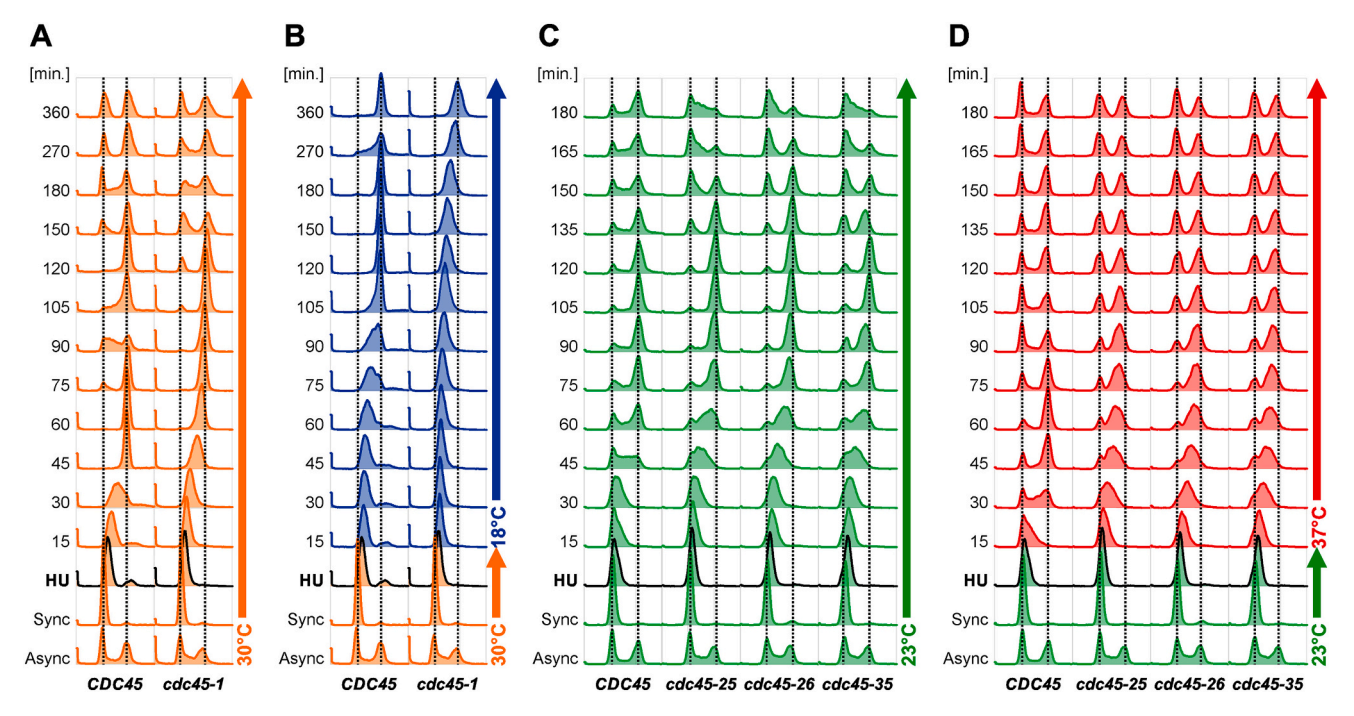


Fig. 5. Cell cycle progression in *cdc45-1* (A, B) and *cdc45-25*, *cdc45-26*, and *cdc45-35* (C, D) mutant cells after synchronization in G1 phase and HU block (black line) at permissive temperature (30 °C in A, B and 23 °C in C, D) allowing initiation of DNA replication. Subsequently, cells were released into a new cell cycle at the permissive (30 °C in A and 23 °C in C) or restrictive (18 °C in B and 37 °C in D) temperature. Samples were taken at indicated time points, and DNA content was analyzed using flow cytometry. More detailed analyzes are shown in Fig. 6.

synthesis by other polymerases (e.g., Pol ζ) or as substrates for homologous recombination. To verify whether this was the case for the four studied cdc45 mutants, we analyzed foci formation by Rfa1, a subunit of RPA that binds ssDNA. For visualization, we used the fusion protein Rfa1-Yfp [36]. Using fluorescence microscopy, we calculated the number of cells with single or multiple foci in cdc45 mutant and wild-type control strains under permissive conditions (Figs. 7 and S4). We found that in the cold-sensitive cdc45-1 cells, over 70 % of cells formed Rfa1 foci, including over 20 % with double foci and over 30 % with three or more foci (Fig. 7). Under the same conditions (30 °C), <63 % of wildtype cells contained Rfa1 foci, with only 36 % showing more than one focus. The results obtained for the three temperature-sensitive mutants cdc45-25, cdc45-26, and cdc45-35 show 53 %-61 % of cells with Rfa1 foci, including 32 %-40 % of cells with two or more foci. In the control wild-type strain, we observed only 40 % of cells with Rfa1 foci, including only 20 % with two or more foci (Fig. 7). Together, these results showed increased ssDNA formation in all tested CDC45 mutants. Therefore, we tested whether the cdc45-1 mutant was dependent on DNA recombination by inactivating the RAD51 or RAD52 genes which encode the main recombinases. Both cdc45-1 $rad51\Delta$ and cdc45-1 $rad52\Delta$ double mutants were viable. Moreover, the deletion of either RAD51 or RAD52 had no effect on the mutation rate of cdc45-1 mutant (Fig. S5).

3.3. CDC45 mutants demonstrate increased mutation rates partially dependent on Pol ζ

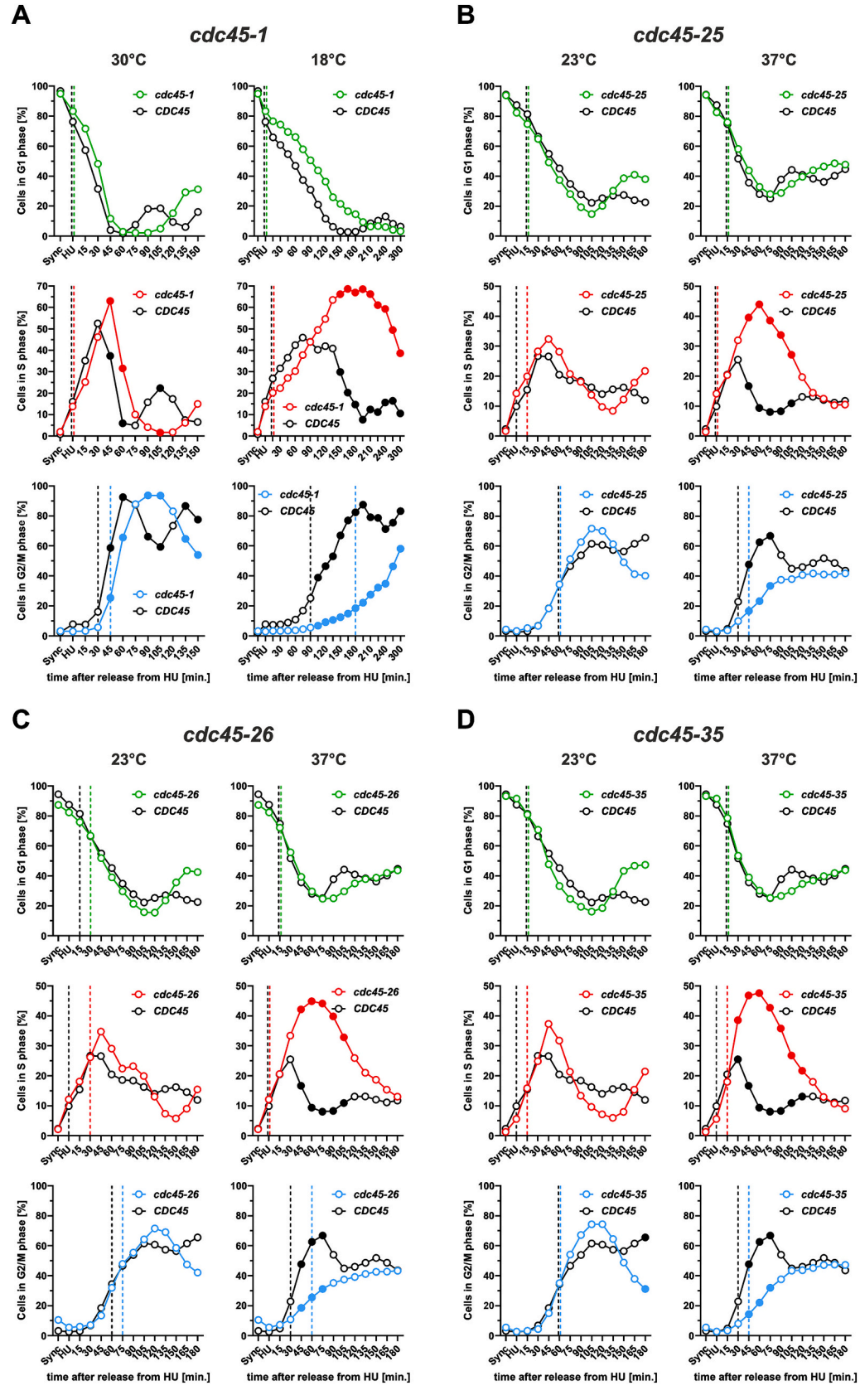
To analyze forward spontaneous mutagenesis levels in *CDC45* mutant cells, we used the *CAN1* locus [40]. The *CAN1* reporter gene facilitates simultaneous testing of different forward mutations such as base substitutions, frameshifts, and more complex mutations [40]. For each mutant, experiments were performed at the permissive temperature. At 30 °C, mutation rates were 101×10^{-8} for wild-type cells and increased to over 175×10^{-8} in cdc45-1 mutant cells (Fig. 8A). At 23 °C, mutation rates were 51×10^{-8} in wild-type cells and increased to over 84×10^{-8} in cdc45-25, cdc45-26, and cdc45-35 cells (Fig. 8A). Together, these results show that the rate of spontaneous mutagenesis at the *CAN1*

locus in the *cdc45* mutant strains was significantly higher than that in the wild-type strains (*p*-values in Table S3), demonstrating that Cdc45 dysfunction enhances spontaneous mutagenesis.

To obtain further insights into the specificity of increased mutagenesis in cdc45-1 mutant cells, we analyzed the sequence of the CAN1 gene in yeast cells from canavanine-resistant colonies (Table S4 and Fig. 8B-D). In cdc45-1 cells, we observed a substantial increase in the frequency of three classes of transversions: GC \rightarrow TA (3.3×), AT \rightarrow TA (2.8×), and GC \rightarrow CG (2.6×) (Fig. 8B). Moreover, previous studies [41–44] and our results obtained for the wild-type strain and rev3 Δ strain presented here (Fig. 8C) show that the GC \rightarrow CG, GC \rightarrow TA, and AT \rightarrow TA transversions are specific to Pol ζ . Therefore, we also analyzed mutation spectra in cdc45-1 cells with the inactivated REV3 gene encoding the catalytic subunit of Pol ζ . The mutation rate in the cdc45-1 $rev3\Delta$ strain was 65 \times 10⁻⁸, demonstrating a significant decrease compared to 175 \times 10^{-8} in cdc45-1 REV3 (Table S4 and Fig. 9A). Rates for specific types of substitutions dropped 20-fold for GC \rightarrow CG, over 6-fold for AT \rightarrow CG, over 5-fold for AT \rightarrow TA, and over 3-fold for GC \rightarrow TA (Fig. 8D). Additionally, the mutation rate for complex mutations, which are also characterized as characteristic of Pol ζ dropped over 26-fold in cdc45-1 $rev3\Delta$ cells compared with cdc45-1 cells (Table S4).

The involvement of Pol ζ in increased mutagenesis was also tested in cdc45-25, cdc45-26, and cdc45-35 cells using strain derivatives with deletion of REV3 (Fig. 9A). In comparison with respective REV3 controls, mutation rates significantly decreased in cdc45-25 $rev3\Delta$, cdc45-26 $rev3\Delta$, and cdc45-35 $rev3\Delta$ cells (by 55 %, 63 %, and 62 %, respectively) (Fig. 9A). This result was similar to that observed in the cdc45-1 $rev3\Delta$ strain (66 %) (Fig. 9A), demonstrating that Pol ζ significantly contributes to increased mutation rates in cdc45 mutant cells.

To analyze whether cdc45 mutations decrease replication fidelity, we inactivated the mismatch repair (MMR) mechanism involved in the repair of base-base mismatches and small insertion-deletion loops made by replicative polymerases [45–47]. This system, temporally coupled with DNA replication, does not correct errors made during translesion DNA synthesis (Pol ζ), DNA repair, or recombination [48]. To inactivate



(caption on next page)

Fig. 6. Cell cycle progression analysis of cdc45-1 (A), cdc45-25 (B), cdc45-26 (C), and cdc45-35 (D) cells at permissive and restrictive temperatures synchronized with α-factor before new cell cycle entry and additionally blocked at the entry of the S phase by hydroxyurea (HU). The analysis is based on flow cytometry profiles shown in Fig. 5. The number of cell in G1, S, and G2/M phases of the cell cycle were calculated for cells synchronized in G1 phase (Sync) and released into a new cell cycle. Samples were taken at indicated time points. Average values were calculated from at least three experiments. Each value is represented by a circle: open circles represent values with no significant differences for the two compared genotypes. Closed circles represent significantly different values ($p \le 0.05$). Dashed lines, colored according to the represented genotype, indicate time points, where the value is significantly different from the value observed at the time of G1 synchronization (Sync). The significance of observed differences was analyzed using a multiple comparison unpaired t-test.

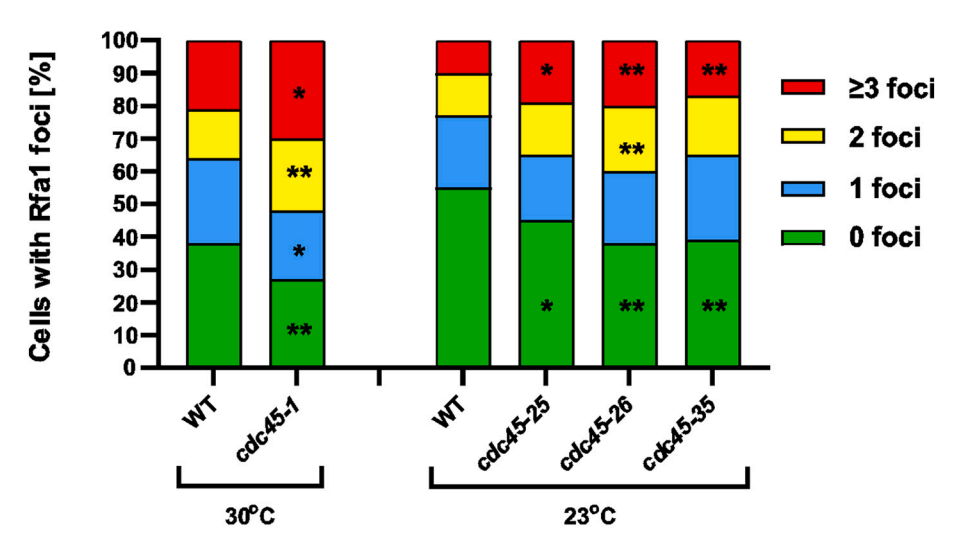


Fig. 7. Visualization of Rfa1-Yfp foci in cdc45-1, cdc45-25, cdc45-26, and cdc45-35 mutant cells. At least 200 cells were analyzed for each of the eight replicates of a given strain (over 1700 in total). The significance of observed differences was analyzed using a multiple comparison unpaired t-test $p \le 0.01$ (**); $p \le 0.05$ (*). Representative images of cells showing Rfa1-Yfp foci are shown in Fig. S4.

MMR in each *cdc45* mutant in the *rev3*Δ background, we deleted the *MSH2* gene encoding the Msh2 protein, which, together with Msh6, binds to the mismatch to initiate the repair mechanism. We analyzed mutation rates at the *his7-2* locus. This reporter allele can revert through one base-pair insertion or a two-base pair deletion in a run of eight A-T base pairs [49]. At 30 °C, the rate of *his7-2* reversion was 50×10^{-8} in *msh2*Δ *rev3*Δ cells, 0.3×10^{-8} in *cdc45-1* cells, and 82×10^{-8} in the triple *cdc45-1 msh2*Δ *rev3*Δ mutants (Fig. 9B). This more-than-additive result shows a synergistic effect of *cdc45-1 msh2*Δ in the Pol ζ-deficient background. A similar effect was observed at 23 °C for the *cdc45-25*, *cdc45-26*, and *cdc45-35* alleles; in the triple mutants, the mutation rates increased from 61×10^{-8} to 91×10^{-8} , 131×10^{-8} , and 99×10^{-8} , respectively (Fig. 9B). These results point out DNA polymerase slippage as a mechanism of Pol ζ-independent mutations introduced during DNA replication in *cdc45* mutant cells.

3.4. Deletion of the DDC1 gene has moderate effects on CDC45 mutants viability and cell cycle progression

Cdc45 dysfunction is thought to affect the rate of DNA replication and thus cell proliferation. However, as shown in a yeast model, Cdc45 is also a targeting factor for Rad53, the main replication checkpoint kinase. After replication checkpoint activation, the phosphorylation of Cdc45 by Rad53 results in their binding and subsequent phosphorylation of Sld3 by the same kinase. This, in turn, inhibits the interaction between Cdc45 and Sld3, facilitating their reactivation after checkpoint inactivation [23]. Besides binding to helicase subunits, Cdc45 also interacts with the catalytic domain of Pol2, the main subunit of Pol ϵ [50,51]. Pol2, together with Dpb2, an essential non-catalytic subunit of Pol ϵ , have been shown to be involved in replication checkpoint activation [52–54]. Therefore, we investigated whether impaired DNA replication checkpoint activation would affect the viability and cellular functions of *CDC45* mutants. The central roles in checkpoint activation are played by Rad53 and Mec1 kinases, which are essential for cell

survival. To preserve the viability of $rad53\Delta$ or $mec1\Delta$ cells, the SML1 gene encoding the ribonucleotide reductase inhibitor must be inactivated, facilitating the increase of the dNTP pool and cell survival [55]. Therefore, we decided to inactivate another element of the DNA replication checkpoint pathway, the Ddc1 protein, a subunit of the 9-1-1 (Ddc1-Rad17-Mec3) checkpoint clamp [56]. DDC1 deletion is synthetically lethal under pri1-2 [56] and dpb2-103 [53] mutation. However, cdc45 $ddc1\Delta$ mutants were viable. More detailed analyses showed a slight decrease of the viability of cdc45-1 $ddc1\Delta$, cdc45-25 $ddc1\Delta$, cdc45-26 $ddc1\Delta$, and cdc45-35 $ddc1\Delta$ cells in comparison to single cdc45 or cdc45 at strains (Fig. S6A). Additionally, a flow cytometry analysis of the DNA content in double mutants showed moderate effects on cell cycle progression in cdc45-1 $ddc1\Delta$ cells (accumulation in G2 phase) as well as in cdc45-25 $ddc1\Delta$, and cdc45-26 $ddc1\Delta$ cells (accumulation in G1 phase) (Fig. S6B).

4. Discussion

Chromosomal DNA replication requires coordinated action of CMG helicases and major DNA polymerases. The correct progression of DNA replication and high fidelity of this process are ensured not only by major DNA polymerases but also by the non-catalytic elements of the replisome. Previously, we have demonstrated the important role of Dpb2 and Psf1 (non-catalytic subunits of DNA polymerase $\boldsymbol{\epsilon}$ and GINS, respectively) in the fidelity of DNA synthesis [35,36,38,43,44,54,57-59]. Cdc45 is an essential protein that, together with the GINS complex and the Mcm2-7 heterohexamer, forms an active CMG helicase, which plays a key role in chromosomal DNA replication. Studies on the non-catalytic Cdc45 protein are of growing interest because defects in same lead to the development of MGORS7 [23-25], craniosynostosis [60], or cancer [28,61]. For example, MGORS7 is an autosomal recessive disease characterized by severe intrauterine and postnatal growth retardation, microcephaly, bilateral microtia, aplasia, and patellar hypoplasia [62,63]. Generally, mutations leading to Meier-Gorlin syndrome

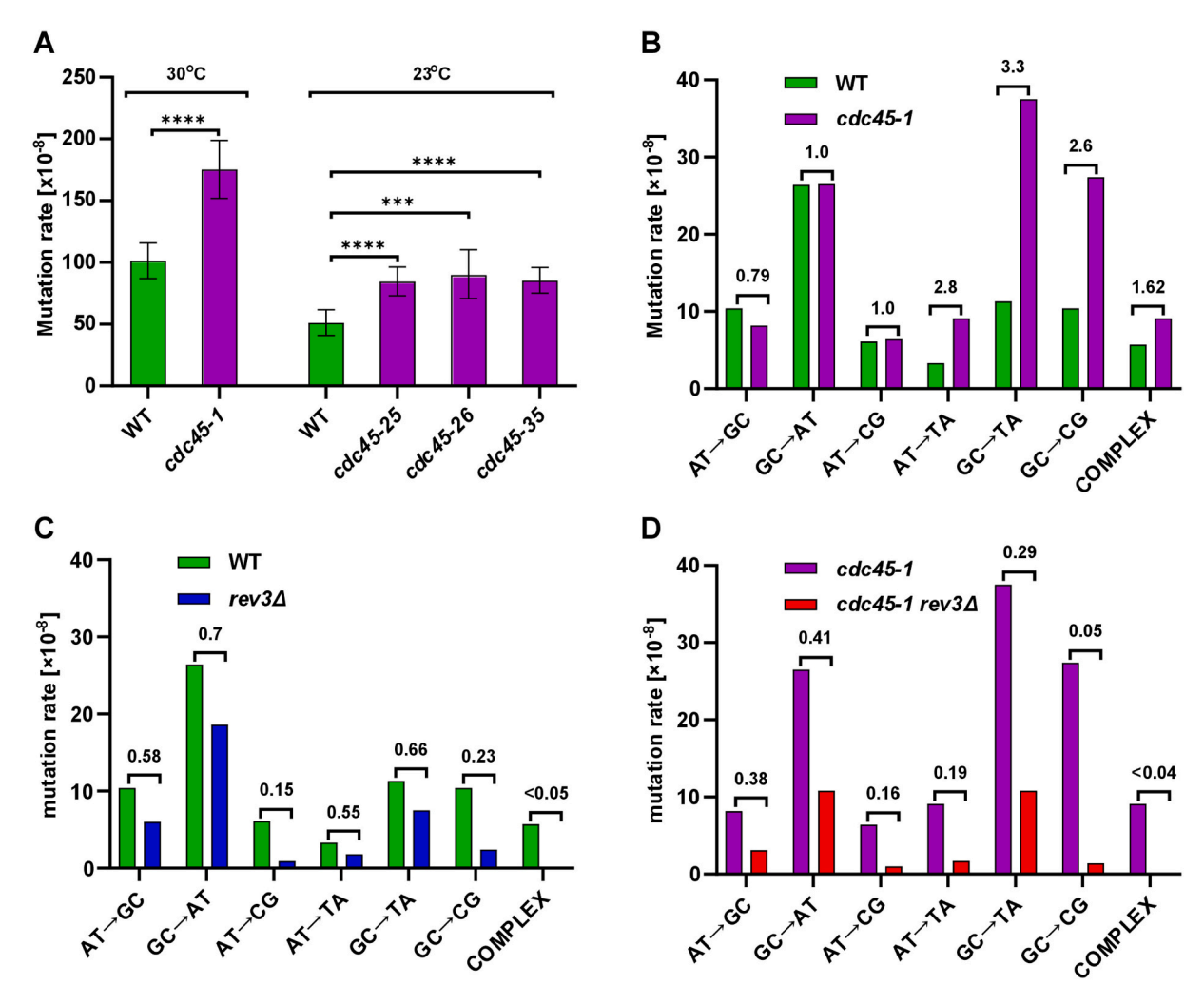


Fig. 8. Spontaneous mutagenesis in the cdc45 strains. (A) Spontaneous mutation rates measured in the cdc45 strains. The presented values were calculated using the maximum likelihood estimate mutation rate calculator (mlemur) [39]. 95 % confidence intervals were calculated from at least ten independent cultures. p-values were adjusted using Benjamini-Hochberg correction $p \le 0.0001$ (****); ≤ 0.001 (***) and are shown in Table S3; (B–D) mutation rates with indicated fold change, calculated for specific mutation types in the CAN1 sequence in yeast strains with the following genotypes: (B) wild-type and cdc45-1 strains; (C) wild-type and $rev3\Delta$ strains; (D) cdc45-1 and cdc45-1 $rev3\Delta$ strains. Mutation spectra for wild-type and $rev3\Delta$ strains were obtained previously [68].

(MGORS) are biallelic and have been identified in pre-RC-encoding genes [64]. In Cdc45, these mutations result in various amino acid substitutions, frameshift or nonsense mutations found throughout the sequence [63], or alter splicing [24]. Variants of the remaining *CDC45* allele in patients with the 22q11.2 deletion were also identified as a causative factor of various anomalies, including craniosynostosis, although independent of MGORS7 [60]. However, the mechanism of this disease is not understood.

Previous studies analyzing *CDC45* mutants focused on cold-sensitive cdc45-1 mutants [14,65,66]. First, it has been demonstrated that when the incubation temperature for cdc45-1 is switched from 30 °C (permissive) to 15 °C (restrictive), mutant cells accumulate partially replicated DNA [14]. When the same temperature shift was performed after cell synchronization in the G1 phase, cdc45-1 cells were unable to enter the S phase for 2–3 h [14]. In a different study published in the same year, the same assay was executed with a temperature shift to 11 °C, again resulting in the accumulation of cells with 1C DNA content [14].

In the present study, we used 18 $^{\circ}$ C as the restrictive temperature and observed a similar effect (Figs. 3B and 4A). After the G1 block, cdc45-1 mutant cells failed to start DNA replication for 2–3 h after release into a new cell cycle at 18 $^{\circ}$ C (Fig. 4A). In contrast, the wild-type cells completed DNA replication under the same conditions. Three new

CDC45 mutants presented in this work, i.e., *cdc45-25*, *cdc45-26*, and *cdc45-35*, are temperature-sensitive, meaning that their growth is inhibited at 37 °C. Thus, they were grown and synchronized with α-factor at 23 °C (permissive temperature) and released from the G1 block at 37 °C (restrictive temperature). All three mutants were unable to start DNA replication at 37 °C, whereas the wild-type strain, under the same conditions, completed DNA replication after 120 min (Figs. 3D and 4B–D).

An alternative to conditional *CDC45* mutants is the heat-inducible degron mutant cdc45-td, which facilitates inactivation of the protein at a specific time [67]. The advantage of this approach is that the protein is fully functional at the permissive temperatures. However, this does not reflect the physiological conditions of cells with amino acid substitutions in protein regions with specific functions (e.g., interactions with other proteins). Nevertheless, the complete inactivation of CDC45 after cell synchronization in the G1 phase results in cell stacking in the G1/early S phase without DNA synthesis [67]. To verify whether Cdc45 defects affect DNA replication initiation or elongation, HU can be used to block DNA synthesis without affecting replication initiation. When cdc45-td cells, after synchronization with α -factor, are transiently incubated with HU at a permissive temperature, heat-induced degradation of Cdc45 results in incomplete DNA replication [67]. This confirms that Cdc45 is also involved in the elongation step of DNA replication.

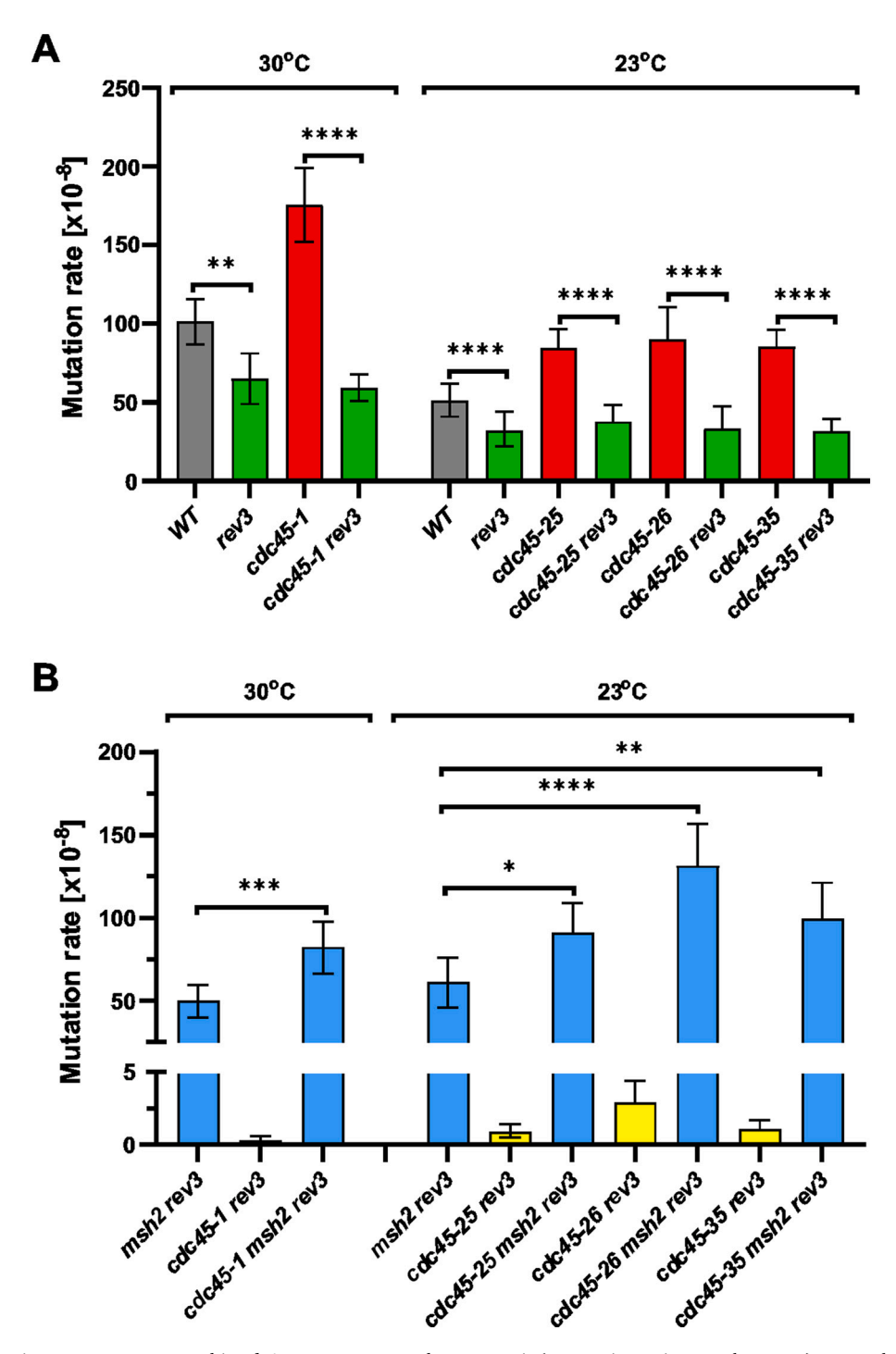


Fig. 9. Spontaneous mutation rates were measured in cdc45 mutants. Forward mutagenesis (canavanine resistance phenotype) was analyzed in the *CAN1* locus in cdc45 strains with $rev3\Delta$ (A). Frameshift mutations (His⁺ phenotype) were scored in $rev3\Delta$ msh 2Δ derivatives of cdc45 mutants (B). The presented values were calculated using the maximum likelihood estimate mutation rate calculator (mlemur) [39]. 95 % confidence intervals were calculated from at least ten independent cultures. The *p*-values were adjusted using the Benjamini-Hochberg correction. $p \le 0.0001$ (****); ≤ 0.01 (**) ≤ 0.05 (*). The *p*-values are shown in Table S3.

In the present study, we observed, that at the permissive temperature (30 °C for *cdc45-1* and 23 °C for *cdc45-25*, *cdc45-26*, and *cdc45-35*), when the time for DNA replication initiation was prolonged through transient HU treatment, all four studied mutants exhibited DNA replication almost as fast as wild-type cells (Figs. 5A, C and 6A–D, left panels). When the same HU block was followed by release at the restrictive temperature (37 °C), mutants *cdc45-25*, *cdc45-26*, and *cdc45-35*, were able to efficiently synthesize DNA, although slightly slower than the wild-type cells (Figs. 5B, D and 6B–D, right panels). However, the *cdc45-1* mutant cells, after 120 min HU block at 30 °C and

release in restrictive conditions (18 °C) showed prolonged progression through the S phase, requiring approximately 90 min more to complete DNA replication (Fig. 6A, right panels). Importantly, when the HU block was reduced to 30 min, *cdc45-1* cells hardly reached the G2 phase even after 4 h. Our results for *cdc45-1* were consistent with the inability to complete DNA replication observed as an effect of induced Cdc45 degradation [67]. Altogether, our results suggest that *cdc45-25*, *cdc45-26*, and *cdc45-35* mutants are defective in replication initiation because temporary HU block facilitates the subsequent rapid completion of DNA replication. In contrast, *cdc45-1*, despite initiation-favorable

conditions, failed to properly proceed with the DNA replication elongation step under restrictive conditions (Fig. 6A), which does not support the conclusions drawn from the data discussed but not shown in a previous study on *cdc45-1* [14].

Our results also demonstrate that DNA synthesis is defective in CDC45 mutant cells, even at permissive temperatures. Both cold- and temperature-sensitive mutants required slightly more time to complete DNA synthesis after S phase entry (Fig. 4). This conclusion is consistent with other results obtained in this study, which showed an increased frequency of ssDNA formation (Fig. 7) as a consequence of defective replisome functioning when CDC45 mutants faced a challenging replication scenario. These defects resulted in increased mutation rates, which almost doubled in cdc45-1 mutant cells and increased by approximately 1.6-fold in cdc45-25, cdc45-26, and cdc45-35 mutant cells (Fig. 8A and Table S3). To the best of our knowledge, this is the first report of increased mutation frequencies in CDC45 mutant cells. As shown in Fig. 9A, the deletion of REV3 significantly reduced the mutation rate in the four CDC45 mutant cells to the level observed in respective control $rev3\Delta$ strains (Table S3). In parallel, our analysis of mutation spectra in cdc45-1 cells in MMR-proficient background when transitions are efficiently repaired, clearly showed an increased incidence of GC \rightarrow CG, GC \rightarrow TA, and AT \rightarrow TA transversions, previously associated mainly with Pol ζ's activity [41–44] (Fig. 8B, C and Table S4). Moreover, in cdc45-1 rev3 Δ cells, mutation rates for these substitutions decreased to the level observed in $rev3\Delta$ cells (Fig. 8C, D). Together, these results show significant participation of Pol ζ in spontaneous mutagenesis in the analyzed CDC45 mutants.

The increased participation in the replication of undamaged DNA of the low-fidelity Pol ζ , which increases the rate of spontaneous mutation, may be due to a phenomenon termed defective-replisome-induced mutagenesis (DRIM) [41]. Previously, we have shown that DRIM could also be promoted by defects in non-catalytic replisome components in *DPB2* and *PSF1* mutants [35,44,68]. The presence of ssDNA in *cdc45* mutants may suggest that under defective CMGE conditions, Pol ζ is recruited to the stalled (impaired) replication forks. Moreover, significantly elevated frameshifts-related mutagenesis observed in Pol ζ -deficient and MMR-deficient background (allowing visualization of replication errors) suggest DNA polymerase slippage as the additional source of mutations introduced during DNA replication in *cdc45* mutant cells (Fig. 9B).

The amino acid substitutions caused by the four mutations analyzed in the current study may cause different defects in Cdc45 function. The cdc45-1 allele, which confers cold sensitivity, encodes a G367D substitution in the CID domain that interacts with the Mcm2 subunit of the DNA helicase core (Fig. 1) as previously suggested [18]. The cdc45-1 was initially isolated as a cold-sensitive cell-division-cycle mutant [21]. Later, it has been shown that *cdc45-1* is synthetically lethal in *mcm2-1*, mcm3-1, and orc2-1 mutants [14]. Among the alleles conferring temperature sensitivity, cdc45-26 encodes a W481R substitution in the RecJ fold that interacts with the Psf1 subunit of GINS (Fig. 1), and cdc45-25 encodes an L131P substitution in DHH, which was suggested to weaken the affinity of Cdc45 to Sld3 [18]. Finally, the cdc45-35 allele encodes a S242P substitution in the helical insertion (specific for Cdc45 and absent in the bacterial RecJ protein), which is involved in replisome interactions, including CMG [18] and Pol2 [50]. Recently, structural studies have demonstrated that this site interacts with Sld3 [69]. Cdc45-Sld3 binding was previously identified as essential for its association with the origin of replication [34] and, as discussed above, for Sld3 phosphorylation upon checkpoint activation [23]. We postulate that the interactions of Cdc45 with other proteins (Mcm2, Psf1, and Sld3) are essential for replisome assembly, which is supported by the observation that DNA replication progression in cdc45-25, -26, and -35 cells is barely affected at the restrictive temperature if the initiation of the process occurs at the permissive temperature (Figs. 5D and 6B-D). Therefore, the cdc45-1 allele differs from the other three alleles because it seems to strongly affect the later steps of DNA replication at the restrictive

temperature after initiating the process under permissive conditions. Although low temperature slowed DNA replication even in wild-type cells by approximately 60 min, the effect observed in *cdc45-1* cells was significantly more pronounced (Fig. 6A).

In summary, in addition to delayed DNA replication in all four mutants analyzed in this study, the effect of these alleles on genome stability was significant. The observed phenotypes can be explained by impaired Cdc45 interactions with other CMGE components resulting in (i) defective replisome assembly and DNA replication initiation, and (ii) defective replisome progression and/or its instability causing DNA polymerase slippage, increased rates of replication errors and incomplete DNA synthesis, generating ssDNA regions, and DNA synthesis rescued by error-prone Pol ζ . These results strongly support the postulated involvement of Cdc45 in DNA replication and maintenance of genome stability.

CRediT authorship contribution statement

Milena Denkiewicz-Kruk: Writing – review & editing, Writing – original draft, Methodology, Investigation, Funding acquisition, Data curation, Conceptualization. Deepali Chaudhry: Writing – review & editing, Investigation, Data curation. Alina Krasilia: Writing – review & editing, Investigation, Data curation. Malgorzata Jedrychowska: Investigation, Data curation. Iwona J. Fijalkowska: Writing – review & editing, Validation, Supervision, Methodology, Formal analysis, Conceptualization. Michal Dmowski: Writing – review & editing, Writing – original draft, Visualization, Validation, Supervision, Methodology, Formal analysis, Data curation, Conceptualization.

Declaration of Generative AI and AI-assisted technologies in the writing process

During the preparation of this work the authors used the Grammarly service in order to proofread the text. After using this tool/service, the authors reviewed and edited the content as needed and take full responsibility for the content of the publication.

Funding

This work was supported by the National Science Centre, Poland (www.ncn.gov.pl) grant no. 2016/21/N/NZ3/03255 to MD-K. The funders had no role in study design, data collection and analysis, decision to publish, or manuscript preparation.

Declaration of competing interest

The authors declare no conflicts of interest.

Acknowledgements

We are grateful to Hiroyuki Araki (NIG, Mishima, Japan) for providing *CDC45* alleles and many valuable discussions. We would also like to thank Maria Furman for excellent technical assistance.

Appendix A. Supplementary data

Supplementary data to this article can be found online at https://doi.org/10.1016/j.bbamcr.2025.119936.

Data availability

Data will be made available on request.

References

- S.P. Bell, A. Dutta, DNA replication in eukaryotic cells, Annu. Rev. Biochem. 71 (2002) 333–374.
- [2] H. Araki, Initiation of chromosomal DNA replication in eukaryotic cells; contribution of yeast genetics to the elucidation, Genes Genet. Syst. 86 (2011) 141–140
- [3] S. Tanaka, R. Nakato, Y. Katou, K. Shirahige, H. Araki, Origin association of Sld3, Sld7, and Cdc45 proteins is a key step for determination of origin-firing timing, Curr. Biol. 21 (2011) 2055–2063.
- [4] R.C. Heller, S. Kang, W.M. Lam, S. Chen, C.S. Chan, S.P. Bell, Eukaryotic origindependent DNA replication in vitro reveals sequential action of DDK and S-CDK kinases. Cell 146 (2011) 80–91.
- [5] K. Labib, Howdo Cdc7 and cyclin-dependent kinases trigger the initiation of chromosome replication in eukaryotic cells? Genes Dev. 24 (2010) 1208–1219.
- [6] S.E. Moyer, P.W. Lewis, M.R. Botchan, Isolation of the Cdc45/Mcm2-7/GINS (CMG) complex, a candidate for the eukaryotic DNA replication fork helicase, Proc. Natl. Acad. Sci. USA 103 (2006) 10236–10241.
- [7] L.D. Langston, D. Zhang, O. Yurieva, R.E. Georgescu, J. Finkelstein, N.Y. Yao, C. Indiani, M.E. O'Donnell, CMG helicase and DNA polymerase ε form a functional 15-subunit holoenzyme for eukaryotic leading-strand DNA replication, Proc. Natl. Acad. Sci. USA 111 (2014) 15390–15395.
- [8] C. Iftode, Y. Daniely, J.A. Borowiec, Replication protein A (RPA): the eukaryotic SSB, Crit. Rev. Biochem. Mol. Biol. 34 (1999) 141–180.
- [9] I. Ilves, T. Petojevic, J.J. Pesavento, M.R. Botchan, Activation of the MCM2-7 helicase by association with Cdc45 and GINS proteins, Mol. Cell 37 (2010) 247–258
- [10] A. Costa, L. Renault, P. Swuec, T. Petojevic, J.J. Pesavento, I. Ilves, K. MacLellan-Gibson, R.A. Fleck, M.R. Botchan, J.M. Berger, DNA binding polarity, dimerization, and ATPase ring remodeling in the CMG helicase of the eukaryotic replisome, Elife 3 (2014) e03273.
- [11] R. Georgescu, Z. Yuan, L. Bai, R. De Luna Almeida Santos, J. Sun, D. Zhang, O. Yurieva, H. Li, M.E. O'Donnell, Structure of eukaryotic CMG helicase at a replication fork and implications to replisome architecture and origin initiation, Proc. Natl. Acad. Sci. USA 114 (2017) E697–E706.
- [12] T. Petojevic, J.J. Pesavento, A. Costa, J. Liang, Z. Wang, J.M. Berger, M.R. Botchan, Cdc45 (cell division cycle protein 45) guards the gate of the eukaryote replisome helicase stabilizing leading strand engagement, Proc. Natl. Acad. Sci. USA 112 (2015) E249–E258.
- [13] K.M. Hennessy, C.D. Clark, D. Botstein, Subcellular localization of yeast CDC46 varies with the cell cycle, Genes Dev. 4 (1990) 2252–2263.
- [14] L. Zou, J. Mitchell, B. Stillman, CDC45, a novel yeast gene that functions with the origin recognition complex and Mcm proteins in initiation of DNA replication, Mol. Cell. Biol. 17 (1997) 553–563.
- [15] I. Bruck, D.L. Kaplan, Cdc45 protein-single-stranded DNA interaction is important for stalling the helicase during replication stress, J. Biol. Chem. 288 (2013) 7550–7563
- [16] L. Sanchez-Pulido, C.P. Ponting, Cdc45: the missing RecJ ortholog in eukaryotes? Bioinformatics 27 (2011) 1885–1888.
- [17] I. Krastanova, V. Sannino, H. Amenitsch, O. Gileadi, F.M. Pisani, S. Onesti, Structural and functional insights into the DNA replication factor Cdc45 reveal an evolutionary relationship to the DHH family of phosphoesterases, J. Biol. Chem. 287 (2012) 4121–4128.
- [18] A.C. Simon, V. Sannino, V. Costanzo, L. Pellegrini, Structure of human Cdc45 and implications for CMG helicase function, Nat. Commun. 7 (2016) 1–15.
- [19] Z. Yuan, L. Bai, J. Sun, R. Georgescu, J. Liu, M.E. O'Donnell, H. Li, Structure of the eukaryotic replicative CMG helicase suggests a pumpjack motion for translocation, Nat. Struct. Mol. Biol. 23 (2016) 217–224.
- [20] L. Pellegrini, Structural insights into Cdc45 function: was there a nuclease at the heart of the ancestral replisome? Biophys. Chem. 225 (2017) 10–14.
- [21] D. Moir, S.E. Stewart, B.C. Osmond, D. Botstein, Cold-sensitive cell-division-cycle mutants of yeast: isolation, properties, and pseudoreversion studies, Genetics 100 (1982) 547–563
- [22] Y.-S. Tak, Regulatory Mechanism of the Initiation of DNA Replication by Cyclindependent Kinase. https://ir.soken.ac.jp/records/992, 2003, pp. 1–68.
- [23] G. Can, A.C. Kauerhof, D. Macak, P. Zegerman, Helicase subunit Cdc45 targets the checkpoint kinase Rad53 to both replication initiation and elongation complexes after fork stalling, Mol. Cell 73 (2019) 562–573.e3.
- [24] A.L. Fenwick, M. Kliszczak, F. Cooper, J. Murray, L. Sanchez-pulido, S.R.F. Twigg, A. Goriely, S.J. Mcgowan, K.A. Miller, I.B. Taylor, C. Logan, W.G.S. Consortium, S. Bozdogan, S. Danda, J. Dixon, S.M. Elsayed, E. Elsobky, A. Gardham, M.J. V. Hoffer, M. Koopmans, et al., Mutations in CDC45, encoding an essential component of the pre-initiation complex, cause Meier-Gorlin syndrome and craniosynostosis, Am. J. Hum. Genet. 99 (2016) 125–138.
- [25] C.Y. Ting, N.S. Bhatia, J.Y. Lim, C.-Y.J. Goh, R.F. Vasanwala, C.C.-P. Ong, W. T. Seow, V.K.-L. Yeow, T.W. Ting, I.S.-L. Ng, S.S. Jamuar, Further delineation of CDC45-related Meier-Gorlin syndrome with craniosynostosis and review of literature, Eur. J. Med. Genet. 63 (2020) 103652.
- [26] Y. Liu, T. Han, Z. Xu, J. Wu, J. Zhou, J. Guo, R. Miao, Y. Xing, D. Ge, Y. Bai, D. Hu, CDC45 promotes the stemness and metastasis in lung adenocarcinoma by affecting the cell cycle, J. Transl. Med. 22 (2024) 1–17.
- [27] X. Zhang, J. Zhou, Y. Wang, X. Wang, B. Zhu, Q. Xing, Elevated CDC45 expression predicts poorer overall survival prognoses and worse immune responses for kidney renal clear cell carcinoma via single-cell and bulk RNA-sequencing, Biochem. Genet. 62 (2024) 1502–1520.

- [28] J. Huang, Y. Li, Z. Lu, Y. Che, S. Sun, S. Mao, Y. Lei, R. Zang, N. Li, S. Zheng, C. Liu, X. Wang, N. Sun, J. He, Analysis of functional hub genes identifies CDC45 as an oncogene in non-small cell lung cancer - a short report, Cell. Oncol. 42 (2019) 571–578.
- [29] J. Sun, R. Shi, S. Zhao, X. Li, S. Lu, H. Bu, X. Ma, Cell division cycle 45 promotes papillary thyroid cancer progression via regulating cell cycle, Tumour Biol. 39 (2017).
- [30] D.C. Amberg, D.J. Burke, J.N. Strathern, Methods in Yeast Genetics: A Cold Spring Harbor Laboratory Course Manual, 2005 edition, 2005. Cold Spring Harbor, NY.
- [31] R.D. Gietz, R.A. Woods, Transformation of yeast by the lithium acetate/single-stranded carrier DNA/PEG method, in: Methods Microbiol, Elsevier, 1998, pp. 53–66.
- [32] J. Sambrook, D.W. Russell, Molecular Cloning: A Laboratory Manual, 3rd ed., 2001.
- [33] Y.I. Pavlov, C.S. Newlon, T.A. Kunkel, Yeast origins establish a strand bias for replicational mutagenesis, Mol. Cell 10 (2002) 207–213.
- [34] Y. Kamimura, Y.S. Tak, A. Sugino, H. Araki, Sld3, which interacts with Cdc45 (Sld4), functions for chromosomal DNA replication in Saccharomyces cerevisiae, EMBO J. 20 (2001) 2097–2107.
- [35] J. Kraszewska, M. Garbacz, P. Jonczyk, I.J. Fijalkowska, M. Jaszczur, Defect of Dpb2p, a noncatalytic subunit of DNA polymerase e, promotes error prone replication of undamaged chromosomal DNA in Saccharomyces cerevisiae, Mutat. Res. 737 (2012) 34–42.
- [36] M. Jedrychowska, M. Denkiewicz-Kruk, M. Alabrudzinska, A. Skoneczna, P. Jonczyk, M. Dmowski, I.J. Fijalkowska, Defects in the GINS complex increase the instability of repetitive sequences via a recombination-dependent mechanism, PLoS Genet. 15 (2019) e1008494.
- [37] A.L. Goldstein, J.H. McCusker, Three new dominant drug resistance cassettes for gene disruption in Saccharomyces cerevisiae, Yeast 15 (1999) 1541–1553.
- [38] M. Dmowski, J. Rudzka, J.L. Campbell, P. Jonczyk, I.J. Fijałkowska, Mutations in the non-catalytic subunit Dpb2 of DNA polymerase epsilon affect the Nrm1 branch of the DNA replication checkpoint, PLoS Genet. 13 (2017) 1–24.
- [39] K. Łazowski, Efficient, robust, and versatile fluctuation data analysis using MLE MUtation Rate calculator (MLEMUR), Mutat. Res. Mol. Mech. Mutag. 826 (2023) 111816.
- [40] C. Chen, R.D. Kolodner, Gross chromosomal rearrangements in Saccharomyces cerevisiae replication and recombination defective mutants, Nat. Genet. 23 (1999) 81–85.
- [41] M.R. Northam, H.A. Robinson, O.V. Kochenova, P.V. Shcherbakova, Participation of DNA polymerase \(\zeta\) in replication of undamaged DNA in Saccharomyces cerevisiae, Genetics 184 (2010) 27–42.
- [42] O.V. Kochenova, R. Bezalel-buch, P. Tran, A.V. Makarova, A. Chabes, P.M. J. Burgers, P.V. Shcherbakova, Yeast DNA polymerase ζ maintains consistent activity and mutagenicity across a wide range of physiological dNTP concentrations. Nucleic Acids Res. 45 (2017) 1200–1218.
- [43] E. Grabowska, U. Wronska, M. Denkiewicz, M. Jaszczur, A. Respondek, M. Alabrudzinska, C. Suski, K. Makiela-Dzbenska, P. Jonczyk, I.J. Fijalkowska, Proper functioning of the GINS complex is important for the fidelity of DNA replication in yeast, Mol. Microbiol. 92 (2014).
- [44] M. Garbacz, H. Araki, K. Flis, A. Bebenek, A.E. Zawada, P. Jonczyk, K. Makiela-Dzbenska, I.J. Fijalkowska, Fidelity consequences of the impaired interaction between DNA polymerase epsilon and the GINS complex, DNA Repair (Amst.) 29 (2015) 23-35
- [45] G.T. Marsischky, N. Filosi, M.F. Kane, R.D. Kolodner, Redundancy of Saccharomyces cerevisiae MSH3 and MSH6 in MSH2-dependent mismatch repair, Genes Dev. 10 (1996) 407–420.
- [46] R.M. Schaaper, The mutational specificity of two Escherichia coli dnaE antimutator alleles as determined from lacI mutation spectra, Genetics 134 (1993) 1031–1038.
- [47] T.A. Kunkel, D.A. Erie, Eukaryotic mismatch repair in relation to DNA replication, Annu. Rev. Genet. 49 (2015) 291–313.
- [48] S.K. Martin, R.D. Wood, DNA polymerase ζ in DNA replication and repair, Nucleic Acids Res. 47 (2019) 8348–8361.
- [49] P.V. Shcherbakova, T.A. Kunkel, Mutator phenotypes conferred by MLH1 overexpression and by heterozygosity for mlh1 mutations, Mol. Cell. Biol. 19 (1999) 3177–3183.
- [50] J. Sun, Y. Shi, R.E. Georgescu, Z. Yuan, B.T. Chait, H. Li, M.E. O'Donnell, The architecture of a eukaryotic replisome, Nat. Struct. Mol. Biol. 22 (2015) 1–9.
- [51] J.C. Zhou, A. Janska, P. Goswami, L. Renault, F. Abid Ali, A. Kotecha, J.F.X. Diffley, A. Costa, CMG–Pol epsilon dynamics suggests a mechanism for the establishment of leading-strand synthesis in the eukaryotic replisome, Proc. Natl. Acad. Sci. 114 (2017) 2017/00530.
- [52] R. Dua, D.L. Levy, J.L. Campbell, Role of the putative zinc finger domain of Saccharomyces cerevisiae DNA polymerase epsilon in DNA replication and the S/M checkpoint pathway, J. Biol. Chem. 273 (1998) 30046–30055.
- [53] M. Dmowski, J. Rudzka, J.L. Campbell, P. Jonczyk, I.J. Fijałkowska, Mutations in the non-catalytic subunit Dpb2 of DNA polymerase epsilon affect the Nrm1 branch of the DNA replication checkpoint, PLoS Genet. 13 (2017) e1006572.
- [54] M. Dmowski, I.J. Fijałkowska, Diverse roles of Dpb2, the non-catalytic subunit of DNA polymerase ε, Curr. Genet. 63 (2017) 983–987.
- [55] X. Zhao, E.G. Muller, R. Rothstein, A suppressor of two essential checkpoint genes identifies a novel protein that negatively affects dNTP pools, Mol. Cell 2 (1998) 329–340.
- [56] M.P. Longhese, V. Paciotti, R. Fraschini, R. Zaccarini, P. Plevani, G. Lucchini, The novel DNA damage checkpoint protein ddc1p is phosphorylated periodically during the cell cycle and in response to DNA damage in budding yeast, EMBO J. 16 (1997) 5216–5226.

- [57] M. Jaszczur, K. Flis, J. Rudzka, J. Kraszewska, M.E. Budd, P. Polaczek, J. L. Campbell, P. Jonczyk, I.J. Fijalkowska, Dpb2p, a noncatalytic subunit of DNA polymerase ε, contributes to the fidelity of DNA replication in Saccharomyces cerevisiae, Genetics 178 (2008) 633–647.
- [58] M. Jaszczur, J. Rudzka, J. Kraszewska, K. Flis, P. Polaczek, J.L. Campbell, I. J. Fijalkowska, P. Jonczyk, Defective interaction between Pol2p and Dpb2p, subunits of DNA polymerase epsilon, contributes to a mutator phenotype in Saccharomyces cerevisiae, Mutat. Res. 669 (2009) 27–35.
- [59] M. Denkiewicz-Kruk, M. Jedrychowska, S. Endo, H. Araki, P. Jonczyk, M. Dmowski, L.J. Fijalkowska, Recombination and pol ζ rescue defective DNA replication upon impaired CMG helicase–pol ε interaction, Int. J. Mol. Sci. 21 (2020) 1–24.
- [60] M. Unolt, M. Kammoun, B. Nowakowska, G.E. Graham, T.B. Crowley, M. S. Hestand, W. Demaerel, M. Geremek, B.S. Emanuel, E.H. Zackai, J.R. Vermeesch, D. McDonald-McGinn, Pathogenic variants in CDC45 on the remaining allele in patients with a chromosome 22q112 deletion result in a novel autosomal recessive condition, Genet. Med. 22 (2020) 326–335.
- [61] Y. Lu, X. Chen, F. Liu, H. Yu, Y. Zhang, K. Du, Y. Nan, Q. Huang, Systematic pancancer analysis identifies CDC45 as having an oncogenic role in human cancers, Oncol. Rep. 48 (2022) 185.
- [62] K.M. Knapp, B. Fellows, S. Aggarwal, A. Dalal, L.S. Bicknell, A synonymous variant in a non-canonical exon of CDC45 disrupts splicing in two affected sibs with Meier-Gorlin syndrome with craniosynostosis, Eur. J. Med. Genet. 64 (2021) 104182.
- [63] E. Nielsen-Dandoroff, M.S.G. Ruegg, L.S. Bicknell, The expanding genetic and clinical landscape associated with Meier-Gorlin syndrome, Eur. J. Hum. Genet. 31 (2023) 859–868.

- [64] L.S. Bicknell, E.M.H.F. Bongers, A. Leitch, S. Brown, J. Schoots, M.E. Harley, S. Aftimos, J.Y. Al-Aama, M. Bober, P.A.J. Brown, H. van Bokhoven, J. Dean, A. Y. Edrees, M. Feingold, A. Fryer, L.H. Hoefsloot, N. Kau, N.V.A.M. Knoers, J. MacKenzie, J.M. Opitz, et al., Mutations in the pre-replication complex cause Meier-Gorlin syndrome, Nat. Genet. 43 (2011) 356–359.
- [65] D. Moir, D. Botstein, Cold-sensitive cell-division-cycle mutants of yeast: isolation, properties, and pseudoreversion studies, Genetics 100 (1982) 547–563.
- [66] J.C. Owens, C.S. Detweiler, J.J. Li, CDC45 is required in conjunction with CDC7/ DBF4 to trigger the initiation of DNA replication, Proc. Natl. Acad. Sci. USA 94 (1997) 12521–12526.
- [67] J.A. Tercero, K. Labib, J.F.X. Diffley, DNA synthesis at individual replication forks requires the essential initiation factor Cdc45p, EMBO J. 19 (2000) 2082–2093.
- [68] E. Szwajczak, I.J. Fijalkowska, C. Suski, The CysB motif of Rev3p involved in the formation of the four-subunit DNA polymerase ζ is required for defective-replisome-induced mutagenesis, Mol. Microbiol. 106 (2017) 659–672.
- [69] H. Li, I. Ishizaki, K. Kato, X. Sun, S. Muramatsu, H. Itou, T. Ose, H. Araki, M. Yao, Structural and functional insights into Cdc45 recruitment by Sld7–Sld3 for CMG complex formation, Elife 81 (2024) 1–25.
- [70] J.S. Lewis, M.H. Gross, J. Sousa, S.S. Henrikus, J.F. Greiwe, A. Nans, J.F.X. Diffley, A. Costa, Mechanism of replication origin melting nucleated by CMG helicase assembly, Nature 606 (2022) 1007–1014.
- [71] M.L. Jones, Y. Baris, M.R.G. Taylor, J.T.P. Yeeles, Structure of a human replisome shows the organisation and interactions of a DNA replication machine, EMBO J. 40 (2021) 1–23.

Milena Denkiewicz-Kruk, Deepali Chaudhry, Alina Krasilia, Malgorzata Jedrychowska, Iwona J. Fijalkowska, Michal Dmowski https://doi.org/10.1016/j.bbamcr.2025.119936

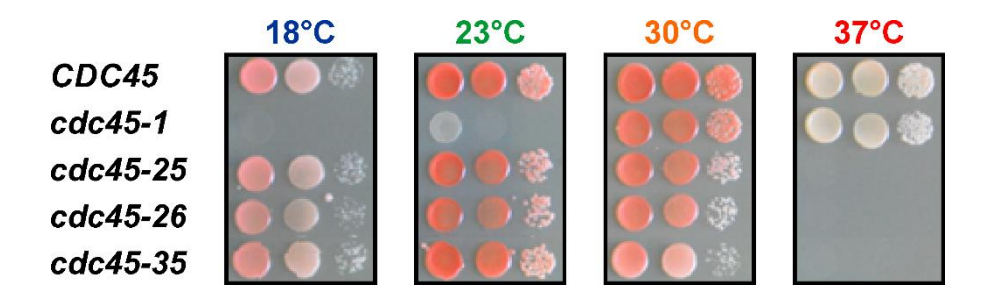


Figure S1. Temperature-sensitivity of *CDC45* **mutants.** Ten-fold serial dilutions of yeast cultures with specified *CDC45* alleles were plated and incubated at indicated temperatures.

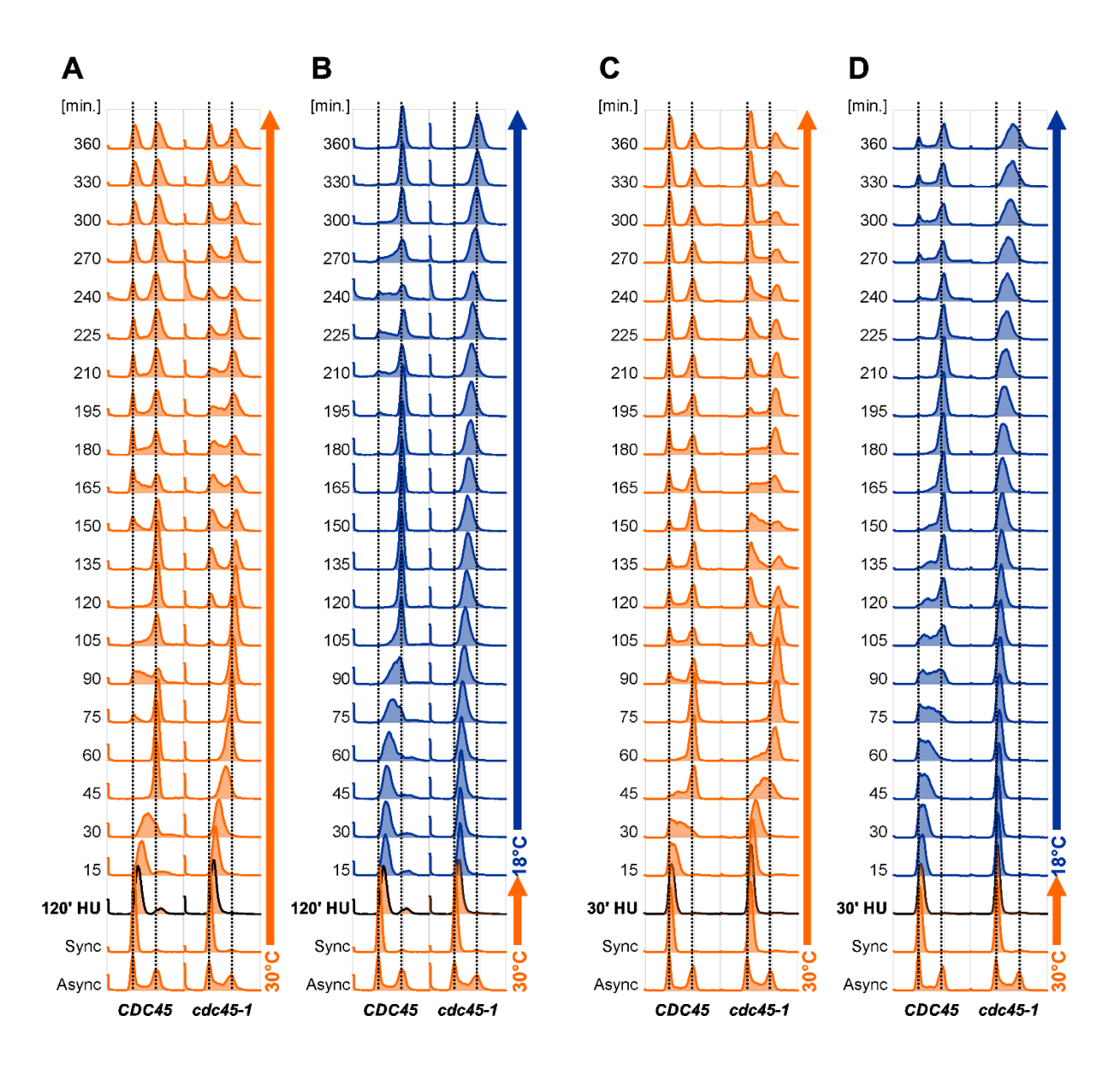


Figure S2. Cell cycle progression of *cdc45-1* mutant cells after synchronization in G1 phase and HU block at permissive temperature (30°C) for 120 min (A-B) or 30 min (C-D) allowing initiation of DNA replication. Subsequently, cells were released into a new cell cycle at the permissive (30°C) (A and C) or restrictive (18°C) (B and D) temperature. Samples were taken at indicated time points, and DNA content was analyzed using flow cytometry. More detailed results, with all time points analyzed, are shown in Figure S3.

Milena Denkiewicz-Kruk, Deepali Chaudhry, Alina Krasilia, Malgorzata Jedrychowska, Iwona J. Fijalkowska, Michal Dmowski https://doi.org/10.1016/j.bbamcr.2025.119936

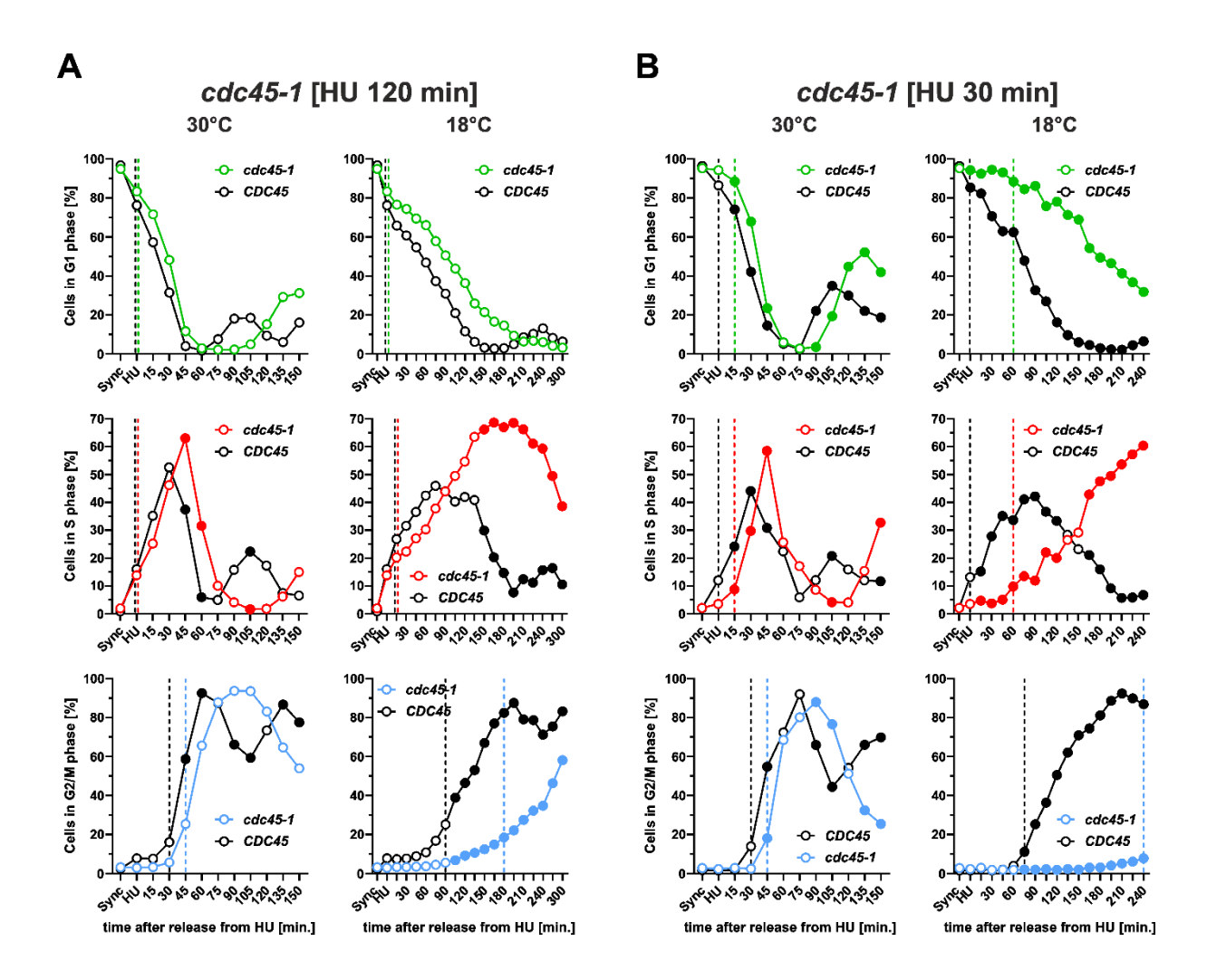


Figure S3. Cell cycle progression analysis of cdc45-1 cells at permissive and restrictive temperatures synchronized with α -factor before new cell cycle entry and additionally blocked at the entry of the S phase by hydroxyurea (HU) for 120 min (A) or 30 min (B). The analysis is based on flow cytometry profiles shown in Figure S2. The number of cell in G1, S, and G2/M phases of the cell cycle were calculated for cells synchronized in G1 phase (Sync) and released into a new cell cycle. Samples were taken at indicated time points. Average values were calculated from at least three experiments. Each value is represented by a circle: open circles represent values with no significant differences for the two compared genotypes. Closed circles represent significantly different values. Dashed lines, colored according to the represented genotype, indicate time points, where the value is significantly different from the value observed at the time of G1 synchronization (Sync). The significance of observed differences was analyzed using a multiple comparison unpaired t-test.

Milena Denkiewicz-Kruk, Deepali Chaudhry, Alina Krasilia, Malgorzata Jedrychowska, Iwona J. Fijalkowska, Michal Dmowski https://doi.org/10.1016/j.bbamcr.2025.119936

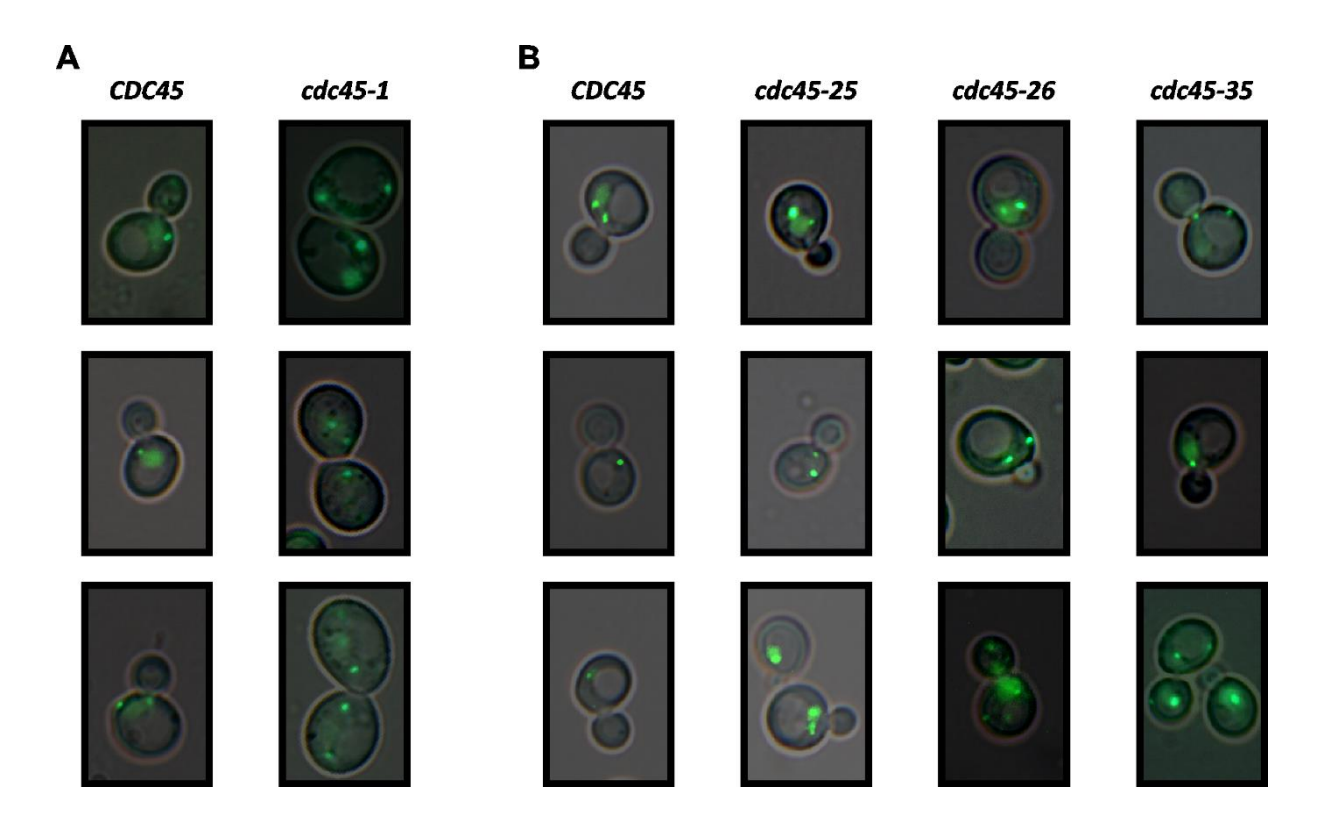


Figure S4. Rfa1-Yfp foci in *cdc45-1, cdc45-25, cdc45-26,* and *cdc45-35* mutant cells cultured at 30°C (A) or 23°C (B).

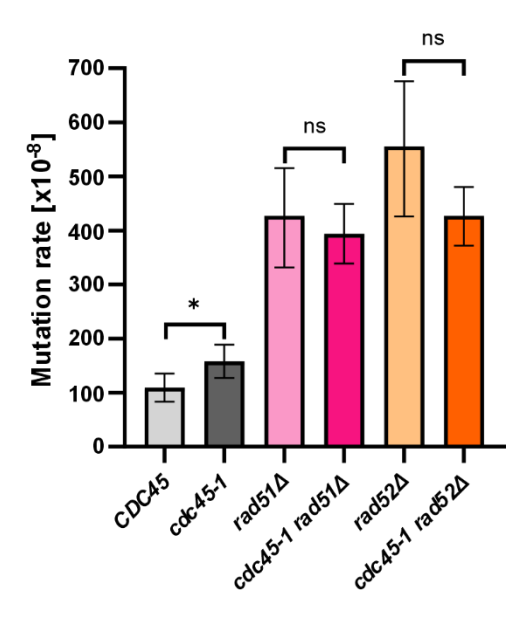


Figure S5. Spontaneous mutation rates were measured in cdc45-1 mutant cells with $rad51\Delta$ or $rad52\Delta$. Forward mutagenesis (Canavanine resistance phenotype) was analyzed in the CAN1 locus. The presented values were calculated using the \underline{m} aximum \underline{l} ikelihood \underline{e} stimate \underline{m} utation \underline{r} ate calculator (mlemur) [39]. 95% confidence intervals were calculated from at least ten independent cultures. The p-values were adjusted using the Benjamini-Hochberg correction were 0.02 (*), 0.55 (ns), and 0.07 (ns).

Milena Denkiewicz-Kruk, Deepali Chaudhry, Alina Krasilia, Malgorzata Jedrychowska, Iwona J. Fijalkowska, Michal Dmowski https://doi.org/10.1016/j.bbamcr.2025.119936

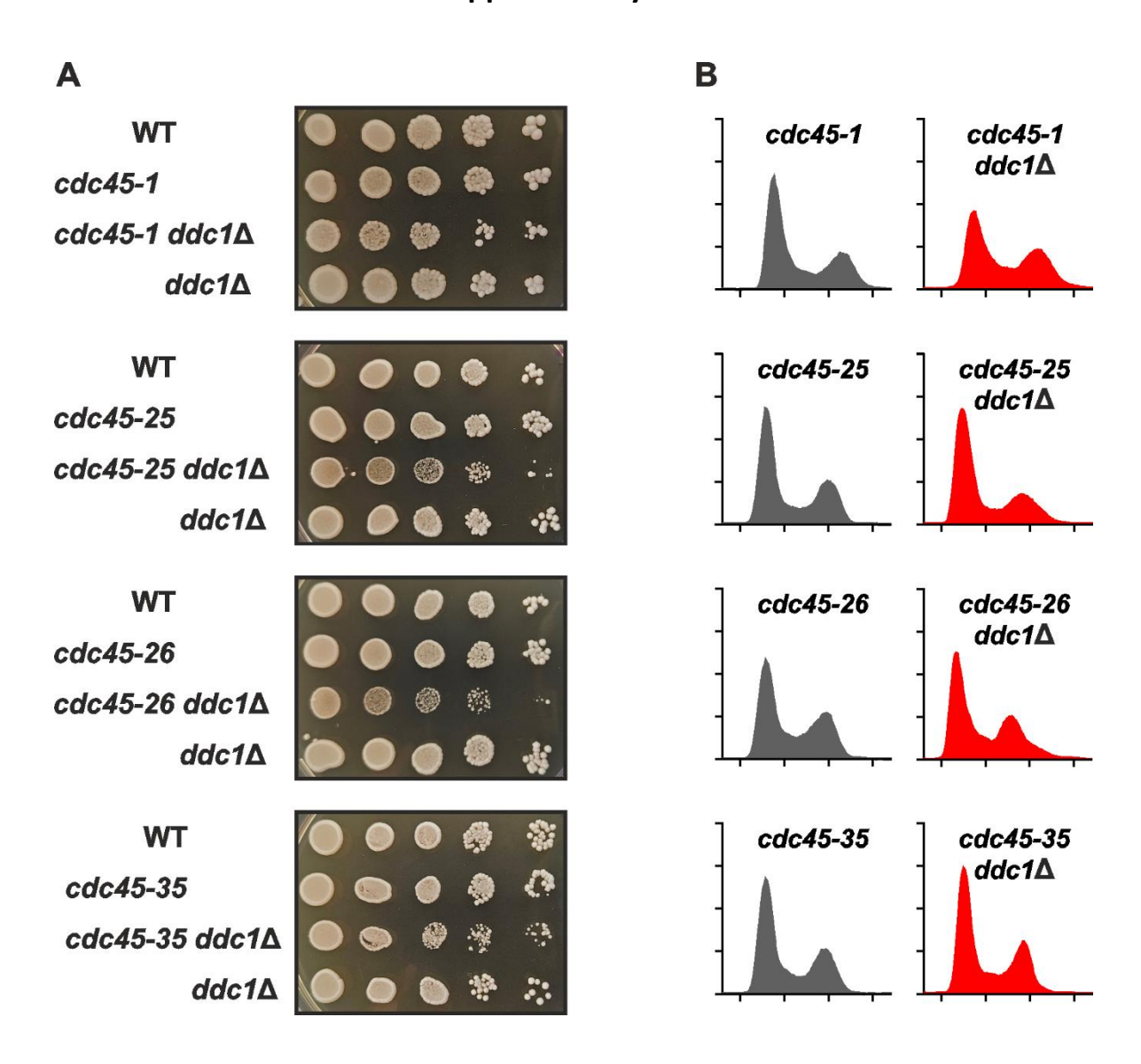


Figure S6. Viability (A) and DNA content profiles (B) of *cdc45* mutant with DDC1 deletion. Exponentially growing cultures of yeast cells of indicated genotypes with similar density were five-fold serially diluted before plating on YPD medium (A). In parallel, cell samples from these cultures were analyzed using flow cytometry (B).

Milena Denkiewicz-Kruk, Deepali Chaudhry, Alina Krasilia, Malgorzata Jedrychowska, Iwona J. Fijalkowska, Michal Dmowski https://doi.org/10.1016/j.bbamcr.2025.119936

Table S1. Yeast strains used in this study.

Strain	Genotype	Source
SC765 ^a	MATa CAN1 his7-2 leu2Δ::hisG ura3Δ trp1-289 ade2-1 lys2ΔGG2899-2900	[43]
Y1050	As SC765, but cdc45-1	This work
Y1051	As SC765, but cdc45-25	This work
Y1052	As SC765, but cdc45-26	This work
Y1053	As SC765, but cdc45-35	This work
Y1054	As SC765, but msh2::NAT1	This work
Y1055	As SC765, but msh2::NAT1 cdc45-1	This work
Y1056	As SC765, but msh2::NAT1 cdc45-25	This work
Y1057	As SC765, but msh2::NAT1 cdc45-26	This work
Y1058	As SC765, but msh2::NAT1 cdc45-35	This work
Y1059	As SC765, but rev3::LEU2	This work
Y1060	As SC765, but rev3::LEU2 cdc45-1	This work
Y1061	As SC765, but rev3::LEU2 cdc45-25	This work
Y1062	As SC765, but rev3::LEU2 cdc45-26	This work
Y1063	As SC765, but rev3::LEU2 cdc45-35	This work
Y1064	As SC765, but (RFA1-YFP, LEU2) cdc45-1	This work
Y1065	As SC765, but (RFA1-YFP, LEU2) cdc45-25	This work
Y1066	As SC765, but (RFA1-YFP, LEU2) cdc45-26	This work
Y1067	As SC765, but (RFA1-YFP, LEU2) cdc45-35	This work
Y1068	As SC765, but rev3::LEU2 msh2::NAT1	This work
Y1069	As SC765, but rev3::LEU2 cdc45-1 msh2::NAT1	This work
Y1070	As SC765, but rev3::LEU2 cdc45-25 msh2::NAT1	This work
Y1071	As SC765, but rev3::LEU2 cdc45-26 msh2::NAT1	This work
Y1072	As SC765, but rev3::LEU2 cdc45-35 msh2::NAT1	This work
Y1001	MATα CAN1 his7-2 leu2Δ::hisG ura3Δ trp1-289 ade2-1 lys2ΔGG2899-2900 rad52::HPH	[59]
Y1002	MATα CAN1 his7-2 leu2Δ::hisG ura3Δ trp1-289 ade2-1 lys2ΔGG2899-2900 rad51::HPH	[59]
Y1084	Derivative of Y1050 and Y1001: MATa/α cdc45-1/CDC45 rad52::HPH/RAD52	This work
Y1085	Derivative of Y1050 and Y1002: MATa/α cdc45-1/CDC45 rad51::HPH/RAD51	This work
Y1086	Derivative of Y1084, cdc45-1 rad52::HPH	This work
Y1087	Derivative of Y1085, cdc45-1 rad51::HPH	This work
Y1079	As SC765, but ddc1::HPH	This work
Y1080	As SC765, but cdc45-1 ddc1::HPH	This work
Y1081	As SC765, but cdc45-25 ddc1::HPH	This work
Y1082	As SC765, but cdc45-26 ddc1::HPH	This work
Y1083	As SC765, but cdc45-35 ddc1::HPH	This work

^a This strain is a derivative of ΔI(-2)I-7B-YUNI300 [33]

Milena Denkiewicz-Kruk, Deepali Chaudhry, Alina Krasilia, Malgorzata Jedrychowska, Iwona J. Fijalkowska, Michal Dmowski https://doi.org/10.1016/j.bbamcr.2025.119936

Table S2. Primers used in this study.

Primer name	Sequence 5'→3'/application
	PCR amplification and DNA sequencing of CAN1 locus
MGCANFF	AAGAGTGGTTGCGAACAGAG
MGCANRR	GGAGCAAGATTGTTGTGGTG
Can_1666	ATATTTGACAGGGAACAAGT
Can_1963	GATGGCTCTTGGAACGGA
Can_2241	TGTCAAGGACCACCAAAG
Can_2465	GTAACTCGTCACGAGAGA
	Gene disruptions
MSH2_UPTEF	CTTTATCTGCTGACCTAACATCAAAATCCTCAGATTAAAAGTATGAGATCTGTTTAGCTTGCC
MSH2_DNTEF	ATTATCTATCGATTCTCACTTAAGATGTCGTTGTAATATTAATTA
	Verification of gene disruptions
MSH2 A	CGTATAAACAAAGCCAAAGACAAGT
MSH2 B	CCCAATTGAATCAAGAAACTCTCTA
MSH2 C	TGAATTGACAGAATTGTCTGAAAAA
MSH2 D	ACATCTCTTGTTTATCCCATCCATA
Msh2_up	TCGGTTCTTACTGCCAAGTG
Msh2_prdw	CATACAGGAGGTGATCCGGT
REV3 A	AATTCTGCCAATCTATTTGATCTTG
REV3 B	TCTGATTTAGAGGATGATCTAACCG
REV3 C	TAAATGAAGACCATAGAGCAGAACC
REV3 D	CACCAGATAGAGTTTTGAACGAAAT
NAT1 UO	ACCGGTAAGCCGTGTCAAG
NAT1 DO	GCTTCGTGGTCGTCTCGTACTC
RAD52 A	GATTCAACAACTCCCTTGGCGTC
RAD52 B	CAACCTTCGATGTATGCAATCCTG
RAD 52 C	CGCGTGAAACCACCAA
RAD52 D	TACGACACATGGAGGAAAAAAC
RAD51 A	CCAATCTAGTTTAGCTATCCTGCAA
RAD51 B	AAAGTGTGACATAGCTGGGACTTAC
RAD51 C	GTAAGTCCCAGCTATGTCACACTTT
RAD51 D	AATTTTTCTCTTCACTCCCCTAAAA
HPH UO	ACAGACGTCGCGGTGAGTTCAG
HPH DO	TCGCCGATAGTGGAAACCGACG
UFddc1_2	GGTGCACTCAATTTGCCGAAAG
DRddc1_2	TAGCGTTCCGGAGTATGTAGG
DDC1UO	TCAGCAGCCGTTAACTGATTCC
DDC1DO	ACACTCTGTGGCTGGAACTC
	PCR amplification and DNA sequencing of cdc45-1, cdc45-25, cdc45-26 and cdc45-35 locus
cdc45_up	AAGCCATGCGAATCCTAC
cdc45_dw	GCCGCGCACAAAATATGG
cdc45_1	CACTAGAGAGAGGCACATA
cdc45_2	GGTACGGTGGATGACACATT
cdc45_3	TCCAACCGGATTACTACCTT
cdc45_4	CGTGGCATTCAACTAGCACA
	Verification of the RFA1-YFP fusion
RFA6231R	ACGGTTCACAATCCCTACAG
RFA7367F	GCCGCAACGCAAACTTCATC
YFP9451R	CTTCGGGCATGGCACTCTTG

Milena Denkiewicz-Kruk, Deepali Chaudhry, Alina Krasilia, Malgorzata Jedrychowska, Iwona J. Fijalkowska, Michal Dmowski https://doi.org/10.1016/j.bbamcr.2025.119936

Table S3. The analysis of statistical significance for data presented in Figures 8 and 9.

		<i>p</i> -value		
		corrected ^a		
	WT	VS	cdc45-1	2.58E-07
	WT	vs	rev3∆	1.22E-03
30°C	cdc45-1	vs	cdc45-1 rev3∆	2.08E-18
30	rev3∆	VS	cdc45-1 rev3∆	5.34E-01
	cdc45-1 rev3∆	VS	cdc45-1 msh2∆ rev3∆	9.15E-30
	msh2∆ rev3∆	VS	cdc45-1 msh2∆ rev3∆	9.56E-04
	WT	VS	cdc45-25	4.82E-05
	WT	VS	cdc45-26	6.04E-04
	WT	VS	cdc45-35	1.16E-05
	WT	VS	rev3∆	2.07E-02
	cdc45-25	VS	cdc45-25 rev3∆	1.43E-08
	cdc45-26	VS	cdc45-26 rev3∆	5.75E-06
23°C	cdc45-35	VS	cdc45-35 rev3∆	3.62E-16
	rev3∆	VS	cdc45-25 rev3∆	5.31E-01
	rev3∆	VS	cdc45-26 rev3∆	9.28E-01
	rev3∆	VS	cdc45-35 rev3∆	9.28E-01
	cdc45-25 rev3∆	VS	cdc45-25 msh2∆ rev3∆	4.28E-24
	msh2∆ rev3∆	VS	cdc45-25 msh2∆ rev3∆	1.61E-02
	cdc45-26 rev3∆	vs	cdc45-26 msh2∆ rev3∆	3.81E-22
	msh2∆ rev3∆	vs	cdc45-26 msh2∆ rev3∆	1.46E-05
	cdc45-35 rev3∆	vs	cdc45-35 msh2∆ rev3∆	7.53E-19
	msh2∆ rev3∆	vs	cdc45-35 msh2∆ rev3∆	7.93E-03

^a p-values were calculated using Benjamini-Hochberg correction for multiple comparisons.

Table S4. Mutation rates are calculated for specific mutation types in the *CAN1* sequence. Mutation spectra for wild-type and $rev3\Delta$ strains were presented previously [68].

	WT		cdc45-1		rev3∆		cdc45-1 rev3∆	
Base substitutions	67.9ª	144 ^b	115.1	126	37.2	124	28.9	83
Transitions	36.8	78	34.7	38	24.6	82	13.9	40
AT→GC	10.4	22	8.2	9	6.0	20	3.1	9
GC→AT	26.4	56	26.5	29	18.6	62	10.8	31
Transversions	31.1	66	80.4	88	12.6	42	15.0	43
AT→CG	6.1	13	6.4	7	0.9	3	1.0	3
AT→TA	3.3	7	9.1	10	1.8	6	1.7	5
GC→TA	11.3	24	37.5	41	7.5	25	10.8	31
GC→CG	10.4	22	27.4	30	2.4	8	1.4	4
Indels	27.8	59	51.2	56	27.9	93	30.3	87
+1	5.2	11	6.4	7	3.3	11	3.5	10
+2	0.5	1	8.2	9	0.3	1	7.3	21
+≥3	1.9	4	5.5	6	5.1	17	5.9	17
-1	12.3	26	24.7	27	7.8	26	8.7	25
-2	5.2	11	5.5	6	6.3	21	3.5	10
≥3	2.8	6	0.9	1	5.1	17	1.4	4
Complex	5.7	12	9.1	10	0.0	0	0.0	0
TOTAL	101.3	215	175.4	192	65.0	217	59.3	170
μ95%–	86.9		151.8		49.1		50.8	
μ95%+	115.8		198.8		81.2		67.9	

^a Mutation rates [Can^R×10⁻⁸] for specific mutation types

^b Number of events identified for given classes

Milena Denkiewicz-Kruk, Deepali Chaudhry, Alina Krasilia, Malgorzata Jedrychowska, Iwona J. Fijalkowska, Michal Dmowski https://doi.org/10.1016/j.bbamcr.2025.119936

- [33] Y.I. Pavlov, C.S. Newlon, T. a. Kunkel, Yeast origins establish a strand bias for replicational mutagenesis, Mol. Cell, 10 (2002) 207–213.
- [39] K. Łazowski, Efficient, robust, and versatile fluctuation data analysis using MLE MUtation Rate calculator (mlemur), Mutat. Res. Mol. Mech. Mutagen., 826 (2023) 111816.
- [43] E. Grabowska, U. Wronska, M. Denkiewicz, M. Jaszczur, A. Respondek, M. Alabrudzinska, C. Suski, K. Makiela-Dzbenska, P. Jonczyk, I.J. Fijalkowska, Proper functioning of the GINS complex is important for the fidelity of DNA replication in yeast, Mol. Microbiol., 92 (2014).
- [59] M. Denkiewicz-Kruk, M. Jedrychowska, S. Endo, H. Araki, P. Jonczyk, M. Dmowski, I.J. Fijalkowska, Recombination and Pol ζ Rescue Defective DNA Replication upon Impaired CMG Helicase—Pol ε Interaction, Int. J. Mol. Sci. 2020, Vol. 21, Page 9484, 21 (2020) 9484.
- [68] E. Szwajczak, I.J. Fijalkowska, C. Suski, The CysB motif of Rev3p involved in the formation of the four-subunit DNA polymerase ζ is required for defective-replisome-induced mutagenesis, Mol. Microbiol., 106 (2017) 659–672.